

I.

AN X-RAY DIFFRACTION STUDY OF THE CRYSTAL STRUCTURE  
OF CYCLOPROPANECARBOHYDRAZIDE

II.

A THEORY OF ISOTROPIC HYPERFINE INTERACTIONS  
IN  $\pi$ -ELECTRON RADICALS

Thesis by

Donald Blair Chesnut

In Partial Fulfillment of the Requirements

For the Degree of

Doctor of Philosophy

California Institute of Technology

Pasadena, California

1958

## ACKNOWLEDGEMENT

It is with pleasure that I acknowledge the direction and guidance of my research advisors, Dr. R. E. Marsh and Dr. H. M. McConnell, whose able leadership has made my years of study at the California Institute of Technology so profitable. It has, indeed, been a privilege to work with men of their scientific caliber and to enjoy their friendship. I particularly want to thank Dr. R. E. Marsh, the chairman of my graduate committee, for his patient and valuable criticism and encouragement and his continued efforts to develop my scientific understanding and ability.

I wish to thank the California Institute of Technology, the E. I. DuPont de Nemours and Company, and the Shell Fellowship Committee for financial assistance during my graduate work.

Finally, it is with a deep sense of gratitude that I thank my family, whose unselfish efforts and encouragement have made possible my educational opportunities, and my wife, whose love and understanding give meaning to my work.

## ABSTRACT

### I.

The crystal structure of cyclopropanecarbohydrazide has been determined and refined using Fourier and least-squares methods. The crystals are monoclinic with  $a_0 = 9.813 \pm 0.003 \text{ \AA}$ ,  $b_0 = 4.847 \pm 0.003 \text{ \AA}$ ,  $c_0 = 11.660 \pm 0.003 \text{ \AA}$ , and  $\beta = 97^\circ 43' \pm 3'$ ; the space group is  $P2_1/c$ , and there are four molecules in the unit cell. The molecules are held together by chains of  $\text{NH} \cdots \text{O}$  hydrogen bonds running parallel to the  $b$  axis and by a network of weak  $\text{NH} \cdots \text{N}$  bonds running along the twofold screw axes which relate the terminal nitrogen atoms. The value of  $1.48 \pm 0.02 \text{ \AA}$  for the C-C distance between the cyclopropane and carbonyl groups suggests the presence of a fairly strong conjugative effect.

## II.

Indirect proton hyperfine interactions in  $\pi$ -electron radicals are first discussed in terms of a hypothetical CH fragment which holds one unpaired  $\pi$ -electron and two  $\sigma$ -CH bonding electrons. Molecular orbital theory and valence bond theory yield almost identical results for the unpaired electron density at the proton due to exchange coupling between the  $\pi$ -electron and the  $\sigma$ -electrons. The unpaired electron spin density at the proton tends to be anti-parallel to the average spin of the  $\pi$ -electrons, and this leads to a negative proton hyperfine coupling constant.

This theory of indirect hyperfine interaction in the CH fragment is generalized to the case of polyatomic  $\pi$ -electron radical systems - e. g., large planar aromatic radicals. In making this generalization there is introduced an unpaired  $\pi$ -electron spin density operator  $\rho_N$ , where N refers to carbon atom N. Molecular orbital theory without configuration interaction gives zero order spin densities  $\rho_N^{(0)}$  which are either positive or zero. If  $\rho_N^{(0)}$  is positive, the calculated proton N hyperfine coupling constant is negative, and negative paramagnetic proton nuclear resonance shifts are predicted in such cases.

Certain aromatic radicals (e. g., odd-alternate aromatics) contain one or more carbon atoms  $\bar{N}$  for which the zero order spin

density is exactly zero,  $\rho_{\bar{N}}^{(0)} = 0$ . In such cases  $\pi$ - $\pi$  configuration interaction gives rise to a first order density at atoms  $\bar{N}$ ,  $\rho_{\bar{N}}^{(1)}$ , which may be positive or negative, leading to negative or positive hyperfine couplings of the protons  $\bar{N}$ .

A previously proposed linear relation between the hyperfine splitting due to proton  $N$ ,  $a_N$ , and the unpaired spin density at  $N$ ,  $\rho_N$ ,

$$a_N = Q \rho_N$$

is derived using molecular orbital theory without  $\pi$ - $\pi$  configuration interaction, assuming the  $\sigma$ - $\pi$  coupling to be first order. It is shown that even when the effects of  $\pi$ - $\pi$  configuration interaction are included in the calculations, the above simple linear relation is still exact, provided the  $\pi$ - $\pi$  configuration interaction is treated as a first order perturbation on the  $\pi$ -part of the wave functions and one assumes the excitation energies of the  $\sigma$ - $\pi$  excited states to be approximately the same.

## TABLE OF CONTENTS

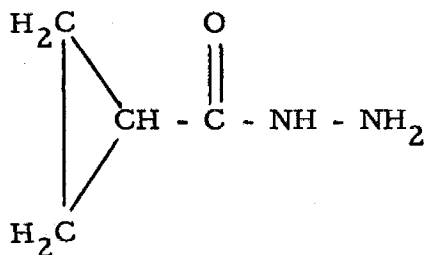
<u>Part</u>	<u>Title</u>	<u>Page</u>
I	An X-ray Diffraction Study of the Crystal Structure of Cyclopropanecarbohydrazide	
	Introduction	1
	Experimental	1
	Determination of the Structure	4
	Discussion	24
	Appendix I	33
	Appendix II	43
	References to Part I	44
II	A Theory of Isotropic Hyperfine Interactions in $\pi$ -Electron Radicals	
	Introduction	46
	The Contact Hyperfine Hamiltonian	47
	$\sigma$ - $\pi$ Electron Interaction in a CH Fragment	50
	Unpaired Electron Distribution and Hyperfine Splittings	56
	Discussion	71
	Appendix I	75
	References to Part II	77
	Propositions	
	References to Propositions	

I.

AN X-RAY DIFFRACTION STUDY OF THE CRYSTAL STRUCTURE  
OF CYCLOPROPANECARBOHYDRAZIDE

INTRODUCTION

Cyclopropanecarbohydrazide (I) contains three structurally interesting groups. First, the cyclopropane ring is of special note



(I)

because in many reactions it tends to behave like an olefinic double bond and to interact with attached conjugated systems. Cyclopropanecarbohydrazide affords a good opportunity for observation of this conjugative power in a system already known to display marked resonance effects. Secondly, one welcomes the chance to observe the amide group - which has been the object of much investigation in these laboratories - in such an unusual environment. The presence of the relatively unstudied hydrazide group represents the third major point of interest.

EXPERIMENTAL

The synthesis of cyclopropanecarbohydrazide has been reported in the literature (1). The crystals used in this investigation were furnished by Professor J. D. Roberts; they were in the form of nearly



square needles, the needle axis being parallel to  $b_0$ . Since the samples exhibited a tendency to sublime at room temperatures, it was necessary to mount them in thin-walled glass tubes during exposures of any length. Samples approximately 1 mm in length and 0.2 x 0.2 mm in cross-section were used for Weissenberg photographs around the  $b$  axis; for photographs about the  $a$  axis, the crystals cut easily perpendicular to the needle axis to form cubes approximately 0.2 mm on an edge.

An approximate density was determined by preparing a solution of acetone and carbon tetrachloride in which a crystal of cyclopropanecarbohydrazide remained suspended. Assuming an ideal solution, an approximate value of 1.24 g/cc was obtained. The density calculated on the basis of four molecules in the unit cell is 1.21 g/cc.

Zero and first layer line Weissenberg photographs about the  $a$  and  $b$  axes yielded the conditions for non-extinction; the absence of  $h0\ell$  reflections with  $\ell$  odd and  $0k0$  reflections with  $k$  odd indicated the space group  $P2_1/c - C_{2h}^5$ . These Weissenberg photographs along with a rotation photograph about the  $b$  axis gave initial values of the cell constants. Accurate values of  $a_0$ ,  $c_0$ , and  $\beta$  were subsequently obtained from a least-squares treatment of several high-angle reflections recorded on a Straumanis-type rotation photograph about the  $b$  axis using Cr K $\alpha$  radiation;  $b_0$  was determined from measurements on an  $0k\ell$  Weissenberg photograph calibrated by the previously determined values for  $c_0$  and  $\beta$ .

The values found and their estimated probable errors are

$$a_o = 9.813 \pm 0.003 \text{ \AA} \quad b_o = 4.847 \pm 0.003 \text{ \AA}$$

$$c_o = 11.660 \pm 0.003 \text{ \AA} \quad \beta = 97^\circ 43' \pm 3'$$

$$\lambda_{\text{Cr K}\alpha} = 2.2909 \text{ \AA}$$

Photographs were taken around the a and b axes (0-3 and 0-4 layer lines respectively) using the multiple-film Weissenberg technique with nickel-filtered copper radiation.\* The maximum Bragg angle observed corresponds to  $\sin \theta_{\text{Cu}} \approx 0.97$ ; due to the rapid fall off of intensity with angle, corresponding to a large temperature factor, only 711 of some 1,300 possible reflections were actually recorded.

The usual Lorentz and polarization corrections were made, and the corrected intensities were normalized to an arbitrary scale by applying the appropriate film factors determined by cross-correlation between the various sets of films. Final values for reflections appearing more than once were obtained by subjectively weighting the separate observations according to the estimated reliability of intensity assignment. Absorption and extinction corrections were neglected although it appears that a number of the larger observed intensities have been reduced by the latter effect.

---

\* The wavelength employed corresponds to the weighted mean wavelength of  $\text{CuK}\alpha_1$  and  $\text{CuK}\alpha_2$  radiation,  $\lambda_{\text{Cu}} = 1.5418 \text{ \AA}$ .

The majority of the calculations were carried out by punched card methods on standard IBM equipment. Two final structure-factor and least-squares calculations were made on the Institute's ElectroData Corporation Datatron digital computer using a program developed by R. A. Pasternak (2) for space groups  $P2$  and  $P2_1$  and modified to accommodate space group  $P2_1/c$ .

### DETERMINATION OF THE STRUCTURE

Projection Studies. A molecular configuration was postulated for which the terminal nitrogen atom was coplanar with the amide group and in the cis configuration with respect to the C-N bond; the plane of the cyclopropane ring was taken to be normal to the plane of the amide group. An examination of packing models showed that placing the proposed molecule in the unit cell such that the C-O bond was parallel to the  $b$  axis (thus allowing a system of  $NH \cdots O$  hydrogen bonds to be formed along the  $b$ -axis) would account very well for the  $b$ -axis identity distance.

Since it seemed very possible that the principal molecular axis was approximately normal to  $[010]$ , it was felt that the initial step in the determination of a trial structure should be a Patterson projection onto (010). The resulting projection is shown in Figure 1. The significant elongation of the peak at the origin was a decisive factor in determining the preliminary trial structure. The length and direction of this peak elongation, along with the very large value of the  $20\bar{2}$  reflection, are consistent with a structure in which the

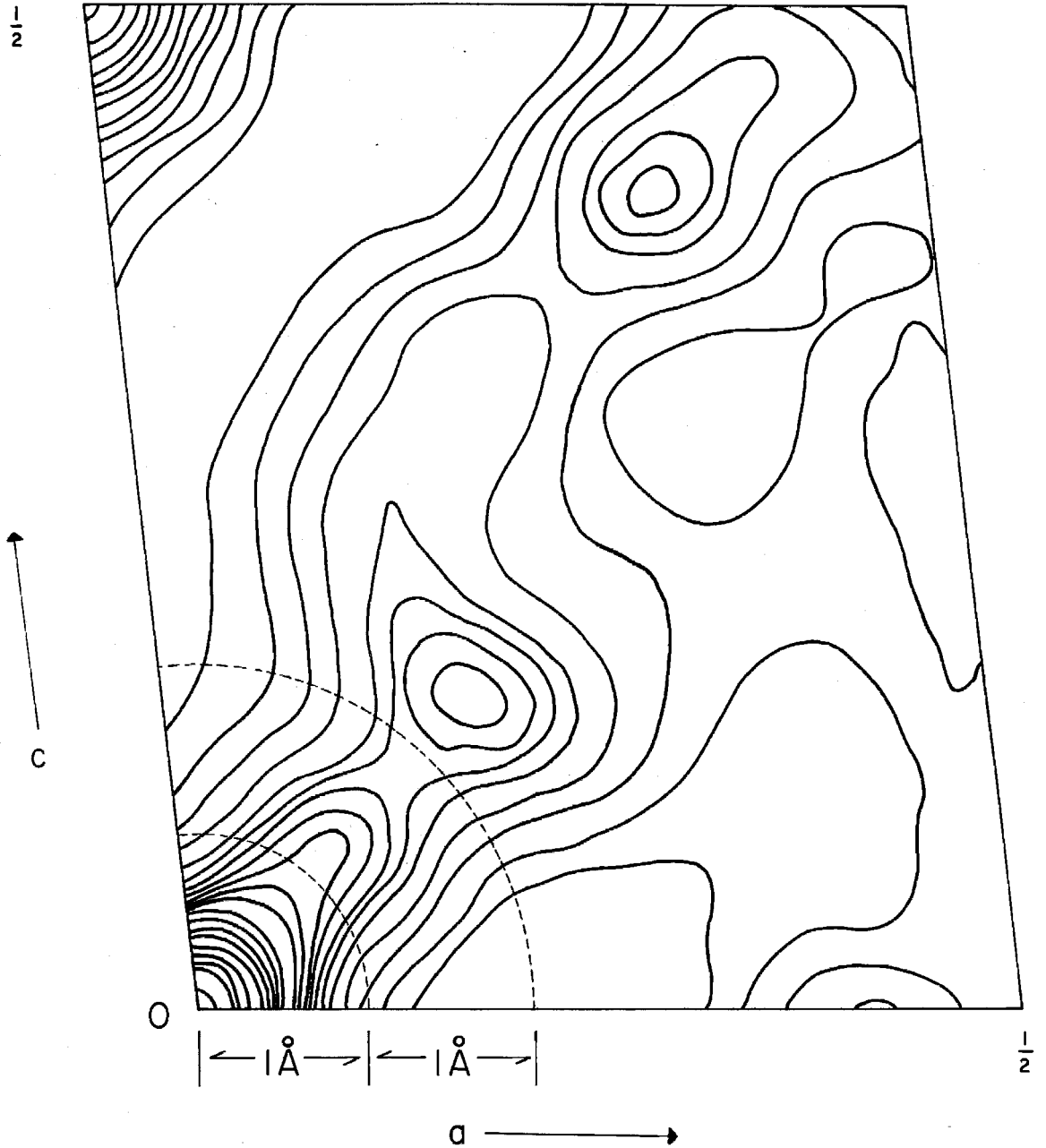


Figure 1. The Patterson projection onto (010).

C-O bond is parallel to  $b_0$ , and the (principal) molecular axis is along the  $[101]$  direction.\*

From the positions of the other peaks on the Patterson map, an estimation of the location of the molecules relative to the symmetry axes could be made. Appropriate trial parameters were then calculated and adjusted until rough agreement was obtained for the stronger  $h0\ell$  terms; the signs of several other terms were determined (in a probabilistic manner) with the aid of the statistical relation - derivable from Harker-Kasper (3) inequalities - that the sign of the product

$$F(\underline{H}) F(\underline{K}) F(\underline{H} + \underline{K})$$

tends to be positive when  $F(\underline{H})$ ,  $F(\underline{K})$ , and  $F(\underline{H} + \underline{K})$  are all large.\*\* When it was felt that the signs of the larger terms were probably correct, an  $h0\ell$  Fourier electron density map was made using fourteen reflections. The resulting projection (Figure 2) was very well resolved considering the fact that so few terms had been used and especially in view of the fact that the molecule had been rotated 180 degrees in the (010) plane about its center. All the atoms were easily located; the assumption that the C-O bond was approximately parallel to the  $b$  axis was borne out by the region of high electron density at the assumed  $C_1$ , O position. The

---

\* See Figure 3 and also Figure 11.

\*\*  $F(\underline{H}) = \sum_j f_j \exp(2\pi i \underline{H} \cdot \underline{r}_j)$ .

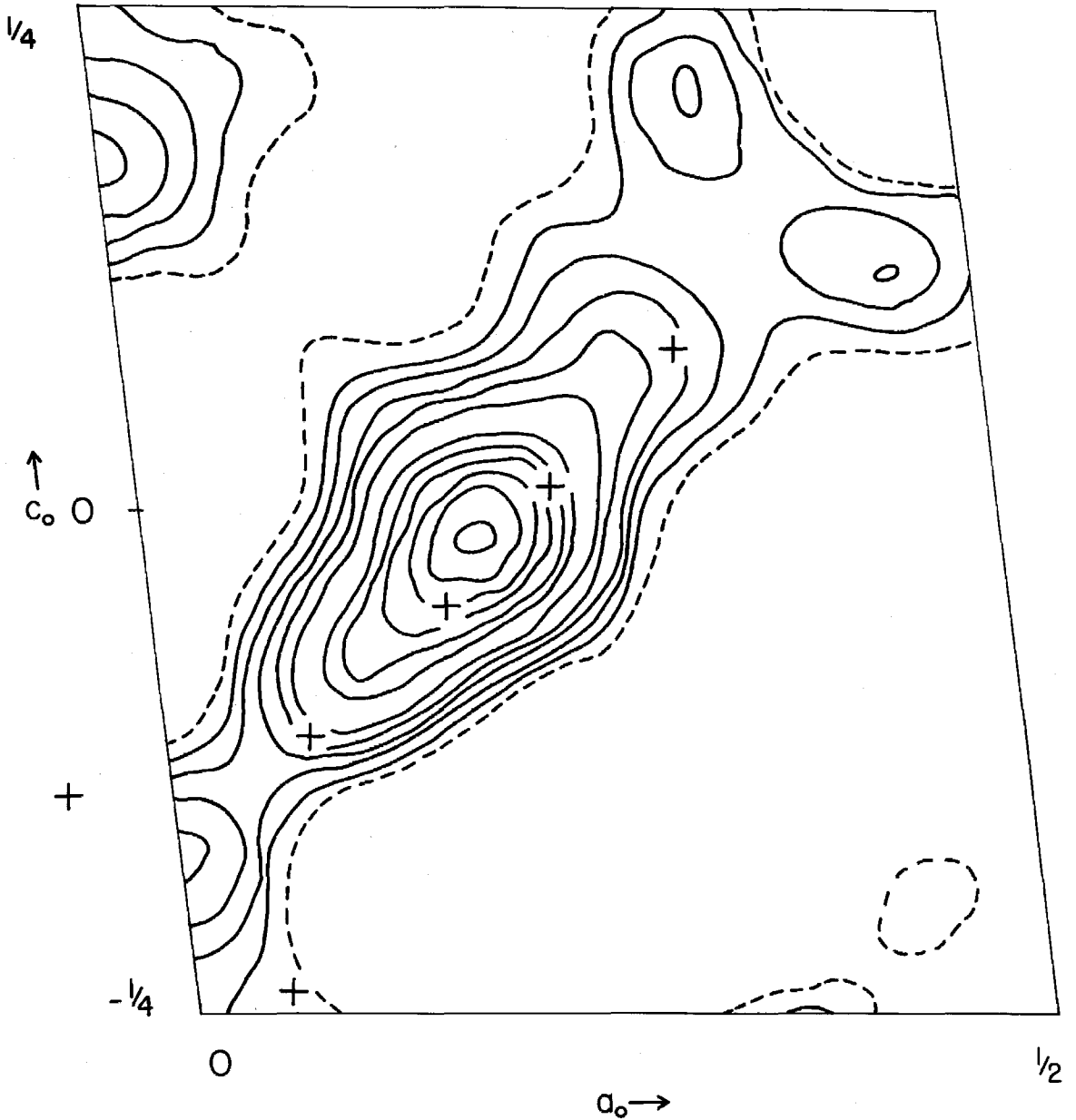


Figure 2. The initial  $h0l$  Fourier electron density map. Crosses indicate the trial structure parameters. The contours are in arbitrary units.

surprisingly good resolution presented strong evidence of the validity of the proposed structure. \*

Table 1 shows the terms that went into this initial Fourier.

---

Table 1

$h0l$	$F_{obs}$	$h0l$	$F_{obs}$
100	+28.3	$30\bar{4}$	-26.7
200	-23.0	$50\bar{4}$	+25.3
$10\bar{2}$	-37.8	$40\bar{6}$	-29.6
$20\bar{2}$	+70.1	302	+41.0
$30\bar{2}$	+52.5	104	+28.4
202	+23.9	506	-26.5
$20\bar{4}$	-58.8	002	-43.3

$F_{obs}$  in electrons per unit cell

---

The final list of structure factors shows that of these fourteen terms the signs of all but the 202 reflection were correct. \*\* The terms in

---

\* At this stage of the investigation, further supporting evidence for the trial structure was found in a preliminary investigation by Jensen and Lingafelter (4) of some n-aliphatic acid hydrazides. The Fourier projections of these compounds were quite similar to that of cyclopropanecarbohydrazide, and the b-axis identity distances were essentially identical, indicating a similarity in packing.

\*\* The signs of the  $h0l$  terms in Table 1 with  $l = 4n + 2$  differ from the final signs given in Appendix I (except in the case of the 202 term which, at this time, was in error) due to the original choice of origin which was displaced by 1/4 in the z direction relative to the correct location. See Appendix II and the section on the (100) projection study.

Table 1 represent half of all terms in the structure having  $|F_{\text{obs}}| > 20.0$  electrons; the  $20\bar{2}$  reflection has the largest magnitude of all observed intensities.

The  $h0\ell$  projection was refined by Fourier and difference maps until the parameter changes led to only very small changes in the overall agreement between observed and calculated structure factors. Even though this zone has the best resolution in the structure, the  $h0\ell$  R-factor at this stage was a rather large 0.38.\*

At this point, attention was focused on the (100) zone. A set of  $y$  parameters was calculated on the basis of expected bond distances and angles, and several Fourier projections were made. These maps had little correspondence to the trial structure, showing the presence of spurious peaks and "holes" of rather large magnitude. A Patterson projection onto (100) was made but its analysis did not reveal the cause of the trouble.

The symmetry of space group  $P2_1/c$  is such that one is unable to distinguish between a twofold screw axis and a center of symmetry when viewing the structure down  $[010]$ . While the wrong choice of origin does not affect the electron density map in the (010) zone, it may result in a completely misleading or meaningless representation of the projected structure in the (100) zone. Since an arbitrary choice of origin had been made in the (010) zonal study, the origin was tentatively shifted by  $1/4$  in  $z$ . The trial parameters

---

\* The final  $h0\ell$  projection, calculated after the complete three dimensional treatment, is shown in Figure 3. The final  $h0\ell$  R-factor was 0.14.



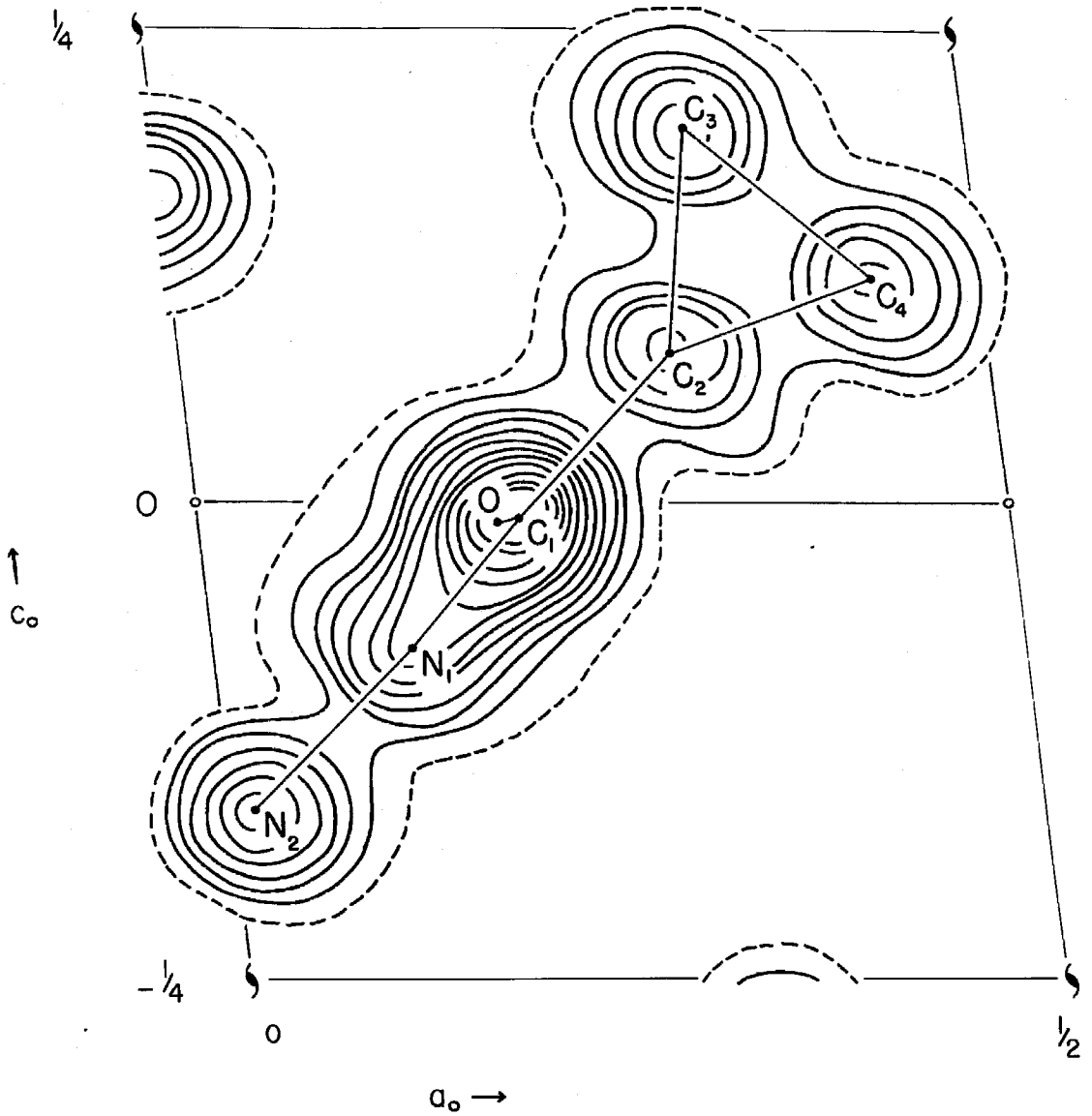


Figure 3. Final  $h0l$  Fourier map. Contours are at approximately one  $e/A^2$  intervals beginning with the zero contour (dashed).

were then adjusted until a set was found which gave the best agreement for most of the larger  $0k\ell$  terms. A subsequent electron density map onto (100) revealed the general features of the molecule, indicating the second choice of origin to be the correct one.

A further problem in this zone became apparent as the projection refined. As can be seen in Figure 4, the projected molecule has a pseudo plane of symmetry due to the similarity of the projected hydrazide and cyclopropane groups. As a result, the agreement of the structure factors for reflections with  $k + \ell$  odd - which were generally weaker than the terms with  $k + \ell$  even - was very sensitive to small changes in the atomic parameters. The first "proper"  $0k\ell$  Fourier projection hinted at this trouble when it presented rather ambiguous information as to which side of the C-O bond the cyclopropane group lay. The choice of the proper alternative removed this ambiguity, subsequent electron density maps revealing the resolved nitrogen atoms. Although this projection provided satisfactory  $y$  parameters for the three dimensional treatment, the discrepancies between the calculated and observed values of the  $k + \ell$  odd terms were not removed by the (100) zonal study and, indeed, were not cleared up until a later analysis of a three dimensional difference map. The two dimensional refinement of this projection was stopped with an  $0k\ell$  R-factor of 0.32.\*

During the projection studies Hoerni and Ibers (5) form factors and isotropic temperature factors were used. McWeeny (6) f-curves were employed for the subsequent three dimensional work

---

\* The final R-factor for this zone was 0.08.

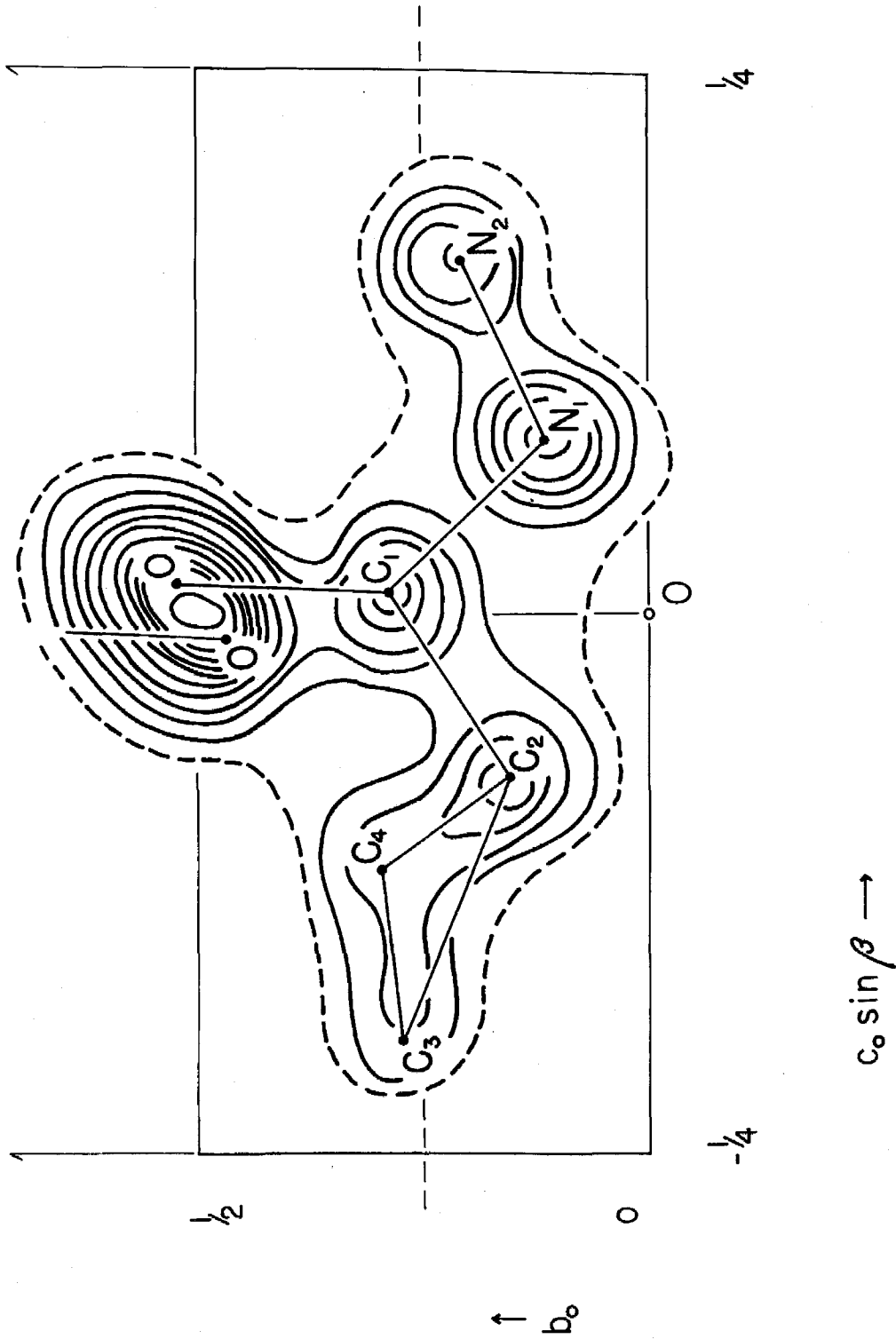


Figure 4. Final  $0 k_L$  Fourier map. Contours are in approximately one  $e/\text{\AA}^2$  intervals beginning with  $3 e/\text{\AA}^2$ . The zero contour is dashed.

with the exception of the final calculations on the Datatron digital computer for which Berghius et al (7) form factors (which are essentially identical to those of Hoerni and Ibers) were used.

The Three Dimensional Study. The three dimensional treatment consisted of about twelve structure-factor least-squares refinements (8) coupled with four three dimensional difference maps and two line Fourier syntheses. The least-squares treatment (in which only the diagonal terms of the normal equations were calculated) progressed very slowly, although the agreement between calculated and observed structure factors continued to improve.\*

In the early stages of the least-squares refinement the question of the location of the origin again arose. A breakdown of the agreement between calculated and observed structure factors showed a considerable dependence of the R-factor on the parity of the index  $l$ .

As can be seen in Table 2, which shows this behavior for an early set of the three dimensional parameters, the reliability index R is much lower for the  $l$ -even terms than for those with

---

\* It is felt that the slow rate of refinement (by the least-squares treatment) was primarily due to large errors in the y parameters. Thus, the y parameter for atom C<sub>4</sub> derived from the (100) projection - 0.683 - differed by about 0.57 Å from the final value. It is apparent that when parameters are in error by a large amount, the shifts indicated by any refinement method in which only the assumed position is inspected will be far too small. In the present case the refinement was speeded by the calculation of several three dimensional difference maps; by this means, not only the slope at the assumed position but also the appearance of neighboring regions was inspected.

Table 2. The dependence of R on the index  $l$  for an early parameter set.

$l$	$\sum /F_{\text{obs}}/$	$\sum /F_{\text{obs}} - F_{\text{cal}}/$	$R = \frac{\sum /F_{\text{obs}} - F_{\text{cal}}/}{\sum /F_{\text{obs}}/}$
0	452	154	0.34
1	579	307	0.53
2	1020	316	0.31
3	540	270	0.50
4	768	284	0.37
5	414	211	0.51
6	551	187	0.34
7	252	131	0.52
8	366	135	0.37
9	162	83	0.51

$l$  odd. In this space group a shift of the origin by  $1/4$  in  $z$  produces changes in the magnitudes of only the  $l$ -odd terms, the  $l$ -even terms being multiplied by either plus or minus one; thus, one might hope to resolve the above difficulty by a shift of origin in the  $z$  direction (see section on (100) zone). However, when such a change was tried, the total  $l$ -odd R-factor increased from 0.52 to 0.70! The anomaly was explained when it was noticed that the nearness to  $1/4$  (or  $3/4$ ) of nearly all the  $y$ -parameters leads to the result (for this space group) that the average  $l$ -even term ought to be larger than the average  $l$ -odd term, an effect which is present in the data shown in Table 2. In an early stage of refinement the larger part of  $\Delta F$  more often than not will come from errors in the positional parameters rather than errors in intensity measurements (which are approximately

proportional to the magnitude of  $F$ ). Thus, each  $\Delta F$  is approximately independent of the magnitude of  $F$ , and the variation of  $\sum /F_{\text{obs}}/$  will lead to the unusual behavior of the R-factor as a function of  $\ell$ . This behavior disappeared as the structure refined.

To aid the rather slow progress of the least-squares, several three dimensional difference maps and line Fourier maps were calculated. The difference maps indicated significant shifts, especially for the  $y$  parameters; these were the least accurate since they had been derived from the  $0k\ell$  Fourier projections which did not give good resolution, that of the ring atoms being particularly poor. The line (one dimensional) Fourier electron density maps were computed principally as checks on the reliability of least-squares results. These are shown in Figures 5 and 6. It can be seen that there is little difference in the final  $y$ -parameters of the  $C_1$ , O, and  $N_2$  atoms and those estimated from the one dimensional maps. The peak densities of the oxygen, nitrogen, and carbon atoms shown in these figures are, as is to be expected, approximately in the ratio 8:7:6.

Toward the end of the refinement a final difference map was computed to confirm the hydrogen-atom positions calculated assuming the usual distances ( $C-H$ ,  $N-H = 1.0 \overset{\circ}{\text{A}}$ ) and tetrahedral or trigonal bond angles. In general, the map showed very few spurious peaks; most of the hydrogens were clearly indicated and checked satisfactorily with the calculated positions. With the exception of the  $N_1$  hydrogen (where it was felt that the indicated position on the difference map was more nearly correct than its calculated position)

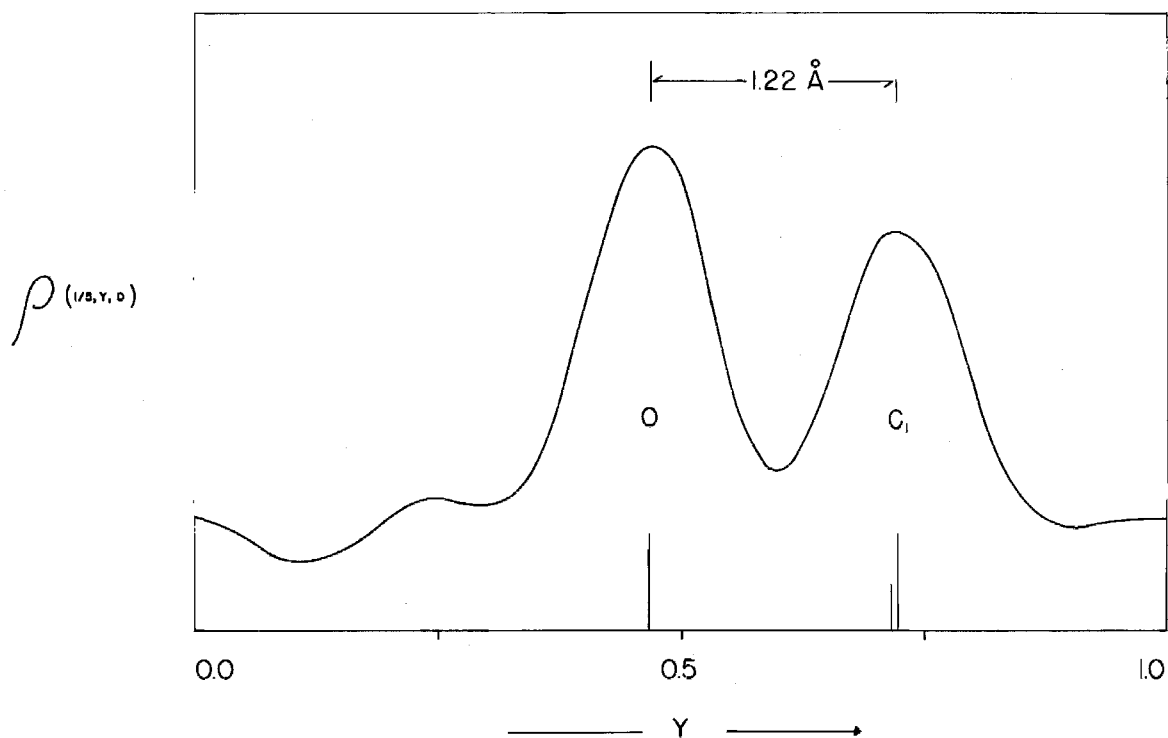


Figure 5. An electron density map along  $(1/5, y, 0)$  showing the  $C_1$  and O atoms. The vertical lines along the abscissa represent the  $y$  parameters measured from the one dimensional map (tall lines) and the final  $y$  parameters (short lines).

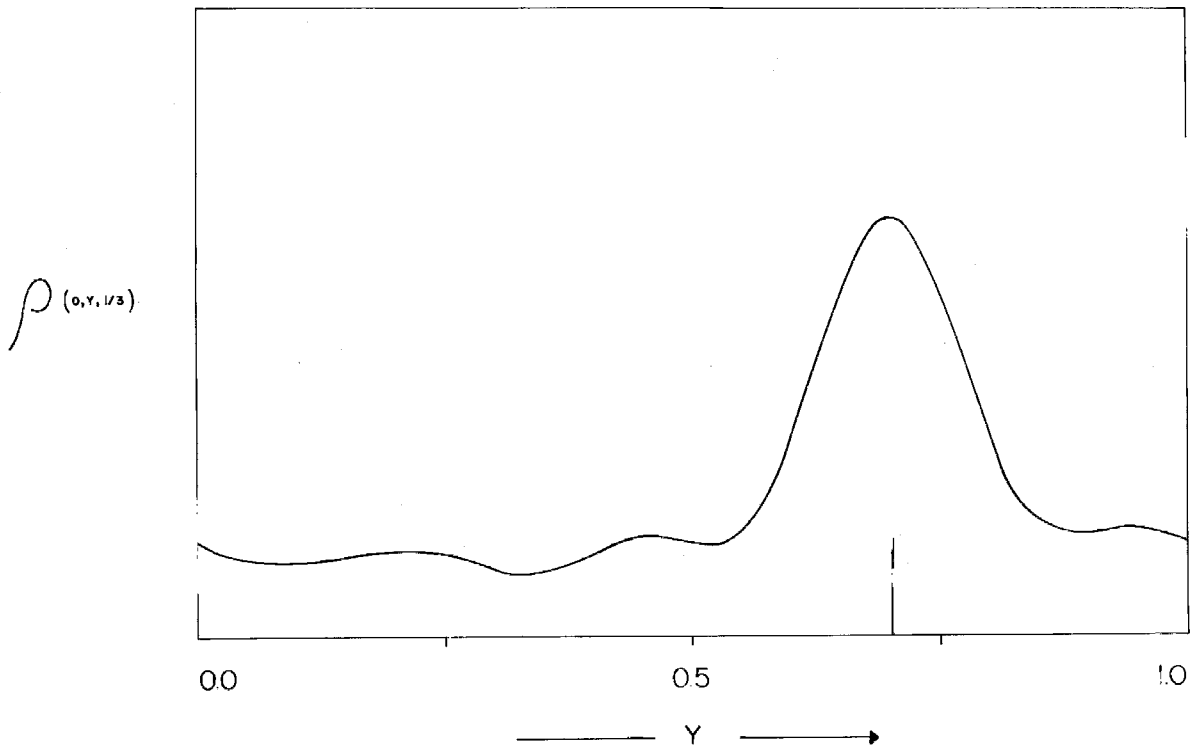


Figure 6. An electron density map along  $(0, y, 1/3)$  showing the  $N_2$  atom. The vertical lines along the abscissa represent the  $y$  parameter measured from the one dimensional map (tall line) and the final  $y$  parameter (short line).



and the  $N_2$  hydrogens (which, of course, could not be calculated a priori), the hydrogen positions given in Table 3 represent the calculated positions. To estimate the positions of the hydrogen atoms bonded to the terminal nitrogen, a section of the map normal to the N-N bond and at a distance of  $0.5 \text{ \AA}$  from  $N_2$  was plotted. This plot, shown in Figure 7, showed two peaks positioned in accordance with a pyramidal configuration. It was interesting to note several other aspects of this particular difference map. Primarily, the peak densities of the hydrogens were rather low, commensurate with the relatively large thermal motions in the structure.\* Furthermore, the best resolution was observed for those hydrogen atoms bonded to heavy atoms having the smaller temperature factors.

The hydrogen atom contributions, including an isotropic temperature factor with  $B = 3.6 \text{ \AA}^2$ , were included in the next structure-factor calculation with a resulting improvement in R of one percent (from 0.142 to 0.131). A least-squares refinement was then computed and indicated that further shifts in the heavy atoms were still needed. These shifts tended to move the atoms away from the hydrogens to which they were bonded. Since anisotropic temperature factors had been introduced prior to including the hydrogen atom contributions in the structure factors, it seemed possible that they might have been affected by overlap of nearby hydrogen atoms. To check on this possible coupling, a second least-squares refinement of the temperature factors was

---

\* The maximum hydrogen peak density was about  $0.8 \text{ e/\AA}^3$ , most others falling around  $0.4 - 0.5 \text{ e/\AA}^3$ .

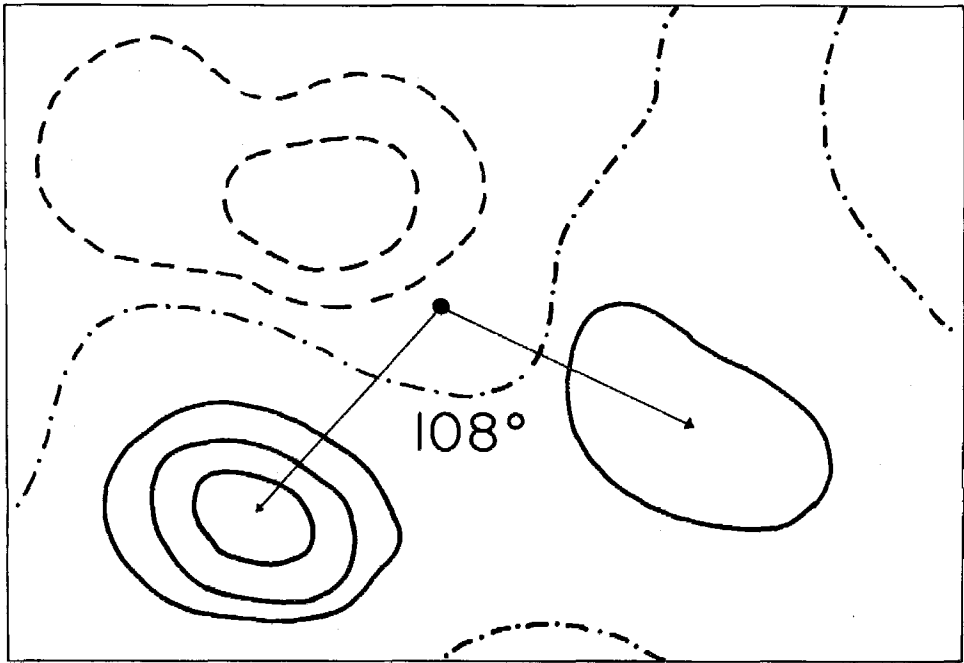


Figure 7. A section of the hydrogen-locating difference map normal to the  $N_2 - N_1$  bond and theoretically containing the two hydrogen atoms bonded to  $N_2$ .

undertaken. Subsequent least-squares on the positional parameters, however, gave negligible shifts.\*

The final positional parameters are given in Table 3. The list of final structure factors is to be found in Appendix I. The final R-factor was 0.13, excluding the unobserved reflections.

---

Table 3  
Final positional parameters (in parameter units)

	x	y	z
C <sub>1</sub>	0.1973	0.7845	0.4908
C <sub>2</sub>	0.3007	0.6492	0.5764
C <sub>3</sub>	0.3263	0.7698	0.6977
C <sub>4</sub>	0.4306	0.8001	0.6181
O	0.1840	0.0332	0.4867
N <sub>1</sub>	0.1227	0.6084	0.4210
N <sub>2</sub>	0.0124	0.7016	0.3374
H <sub>1</sub> (C <sub>2</sub> )	0.301	0.435	0.568
H <sub>2</sub> (C <sub>3</sub> )	0.334	0.647	0.772
H <sub>3</sub> (C <sub>3</sub> )	0.265	0.940	0.721
H <sub>4</sub> (C <sub>4</sub> )	0.521	0.691	0.636
H <sub>5</sub> (C <sub>4</sub> )	0.453	0.984	0.585
H <sub>6</sub> (N <sub>1</sub> )	0.133	0.409	0.438
H <sub>7</sub> (N <sub>2</sub> )	-0.067	0.815	0.367
H <sub>8</sub> (N <sub>2</sub> )	0.021	0.877	0.286

---

\* As the structure approached convergence, a weight of

$$\omega = \frac{1}{F^2} \quad F \geq 4 F_{\min}$$

$$\omega = \frac{1}{4 F_{\min} F} \quad F \leq 4 F_{\min}$$

was used in the least-squares treatment. Unobserved reflections and reflections suffering from extinction were given zero weight.

Temperature Factors. In the early stages of refinement a single isotropic or a single average anisotropic temperature factor was used to compensate for the thermal motion of the atoms. When it was felt that the errors in the calculated structure factors due to a temperature anisotropy were comparable with those due to the displacement of the atomic positions from their true locations, individual anisotropic temperature factors of the form

$$T_i = \exp(-\alpha_i h^2 - \beta_i k^2 - \gamma_i l^2 - \delta_i hl)$$

were introduced. The form of the above expression indicates that one axis of the temperature factor ellipsoid was taken to be parallel to the b axis. This simplification was made after studying a three dimensional difference map which indicated that such an approximation would be justified. The temperature factors were calculated using a least-squares method (9) and compared favorably with rough values computed from the difference map itself (10). The temperature parameters underwent one least-squares refinement prior to the final structure-factor calculations; this final set is listed in Table 4.

In order to better picture the physical effects from which these temperature-factor parameters are derived, the mean square displacements ( $\bar{u}^2 = B/8\pi^2$ ) of each atom along the three principal axes of motion (the major axes of the temperature factor ellipsoid) were calculated (11). These mean square displacements and their directions are given in Table 5 and are represented schematically in Figure 8. As expected, the largest thermal motion is that of the oxygen atom in directions normal to the C-O bond.

Table 4

## Temperature parameters

Anisotropic temperature factors in the expression

$$T_i = \exp \left\{ - \left[ \alpha_i h^2 + \beta_i k^2 + \gamma_i l^2 + \delta_i h l \right] \right\}$$

All values have been multiplied by  $10^3$ 

	$C_1$	$C_2$	$C_3$	$C_4$	O	$N_1$	$N_2$
$\alpha$	13.8	12.2	17.5	8.7	21.5	15.8	15.8
$\beta$	18.5	33.0	83.2	58.3	17.0	27.9	39.7
$\gamma$	9.5	8.9	7.1	10.4	14.0	8.2	6.4
$\delta$	0.1	- 4.5	- 2.1	- 3.2	- 6.0	- 1.1	- 6.3

Table 5

## Temperature parameters

Values of  $\bar{u}^2$  ( $\text{\AA}^2$ ) for the major axes of the temperature factor ellipsoids.  $\tau_1$  represents the larger of the two axes  $\tau_1$  and  $\tau_2$ , which lie in the ac plane;  $\tau_b$  is the axis parallel to  $b_0$ .  $\angle(\tau_2, a)$  is the angle the axis  $\tau_2$  makes with the lattice vector  $\underline{a}_0$ .

	$C_1$	$C_2$	$C_3$	$C_4$	O	$N_1$	$N_2$
$\tau_1$	0.075	0.083	0.091	0.080	0.134	0.083	0.094
$\tau_2$	0.058	0.041	0.044	0.036	0.072	0.051	0.032
$\tau_b$	0.022	0.039	0.099	0.069	0.020	0.033	0.047
$\angle(\tau_2, a)$	$52^\circ$	$48^\circ$	$73^\circ$	$29^\circ$	$53^\circ$	$69^\circ$	$65^\circ$

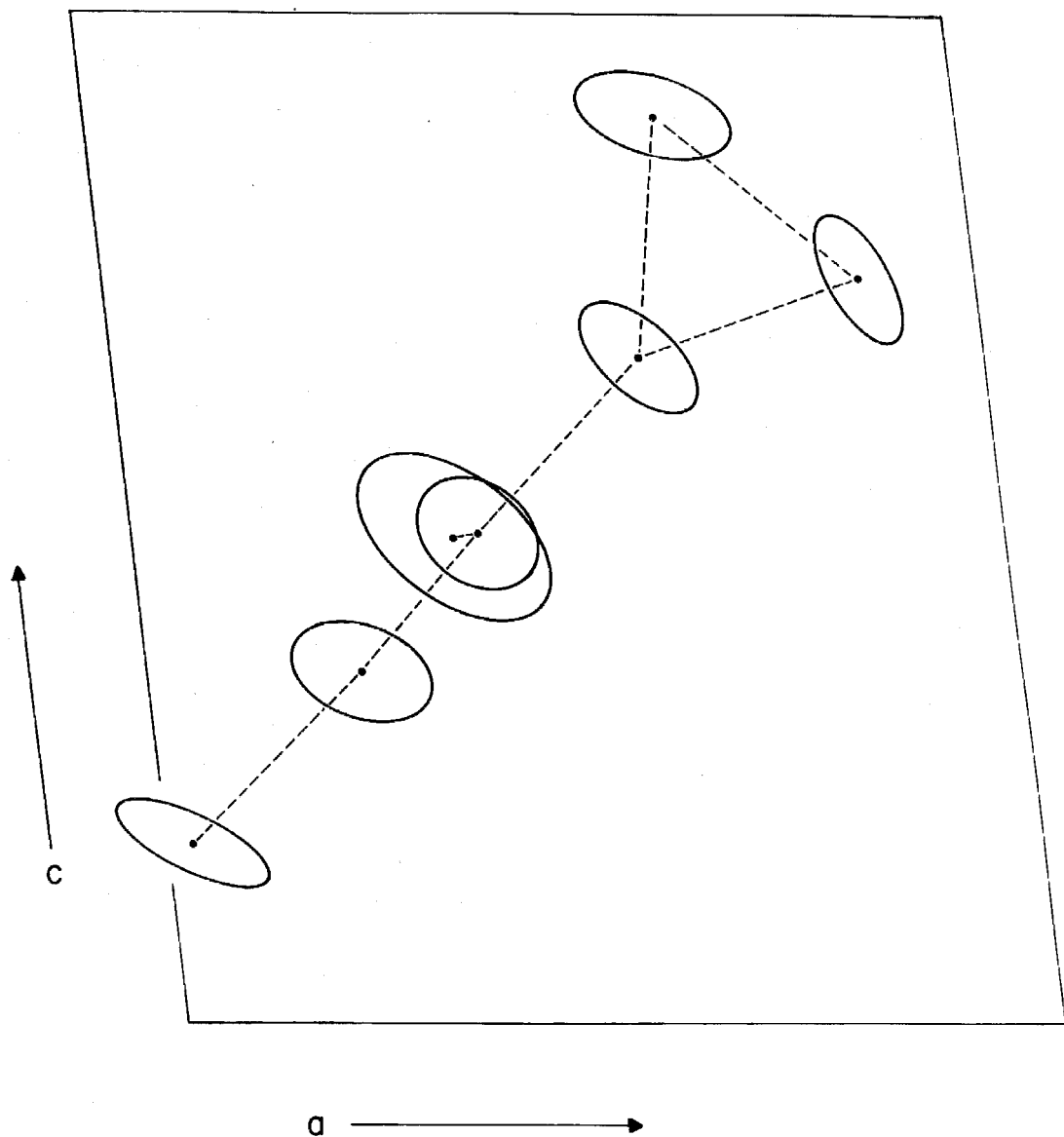


Figure 8. A schematic representation of the relative magnitudes of thermal anisotropy in the cyclopropanecarbohydrazide molecule viewed down  $[010]$ . The magnitudes of the  $\bar{u}^2$ 's have been increased by a factor of approximately 5.3 relative to the interatomic distances.

DISCUSSION

Accuracy of the Structure. The standard deviations of the atomic parameters were calculated using the weighted residuals from the least-squares treatment; the average value was  $0.010 \text{ \AA}$ . This leads to an average standard deviation of about  $0.015 \text{ \AA}$  in the bond distances and of about two degrees in the bond angles. It is felt that systematic errors in intensities might increase these uncertainties to  $0.02 \text{ \AA}$  and three degrees.

Bond Distances and Angles. Interatomic distances and angles calculated on the basis of Table 3 are listed in Table 6 and are shown in Figure 9.

---

Table 6  
Bond distances and angles

bond	d( $\text{\AA}$ )	angle	(degrees)
C <sub>1</sub> - C <sub>2</sub>	1.478	C <sub>2</sub> C <sub>3</sub> C <sub>4</sub>	59.7
C <sub>2</sub> - C <sub>3</sub>	1.520	C <sub>3</sub> C <sub>4</sub> C <sub>2</sub>	61.5
C <sub>2</sub> - C <sub>4</sub>	1.493	C <sub>4</sub> C <sub>2</sub> C <sub>3</sub>	58.8
C <sub>3</sub> - C <sub>4</sub>	1.478	N <sub>2</sub> N <sub>1</sub> C <sub>1</sub>	121.3
C <sub>1</sub> - O	1.213 *	N <sub>1</sub> C <sub>1</sub> O	124.5
C <sub>1</sub> - N <sub>1</sub>	1.329	O C <sub>1</sub> C <sub>2</sub>	121.9
N <sub>1</sub> - N <sub>2</sub>	1.429	N <sub>1</sub> C <sub>1</sub> C <sub>2</sub>	113.6
		C <sub>1</sub> C <sub>2</sub> C <sub>3</sub>	118.3
		C <sub>1</sub> C <sub>2</sub> C <sub>4</sub>	118.8
		C <sub>1</sub> C <sub>2</sub> M	123.1

\* See Discussion

---

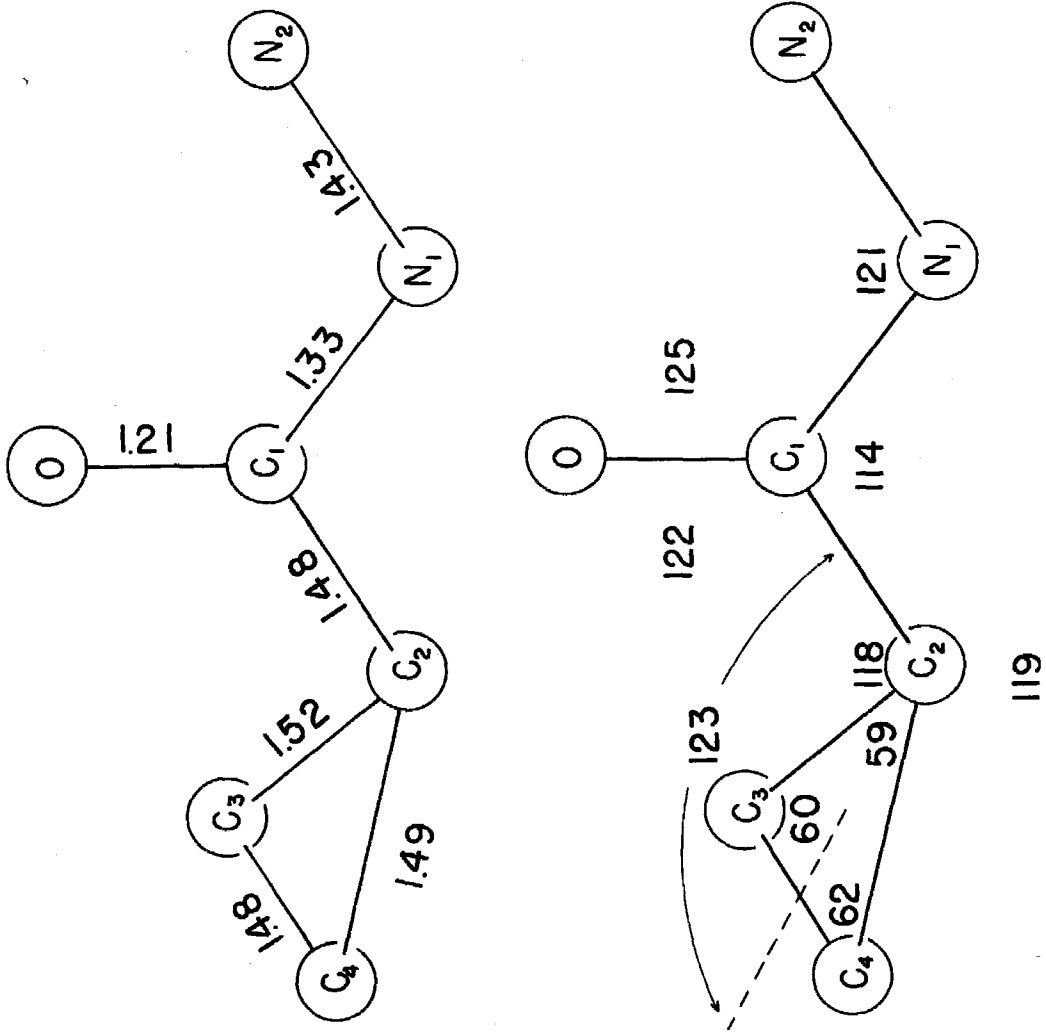


Figure 9. Bond distances and angles in cyclopropanecarbohydrazide.



A simple treatment of the temperature factors (12) indicates a shortening of the  $C_1$ -O bond length by approximately  $0.02 \text{ \AA}$  due to the differences in the magnitudes of the anisotropic motion of these two atoms. Thus the "real"  $C_1$ -O distance is approximately  $1.23 \text{ \AA}$ . It is felt that similar corrections to the other bond lengths are not justified.

The dimensions of the amide group have not been appreciably affected by the presence of the terminal nitrogen or the conjugative effect of the cyclopropane ring; the angles and distances are essentially the same as those found in simple peptides (13). The  $C_2C_1ON_1$  group is planar with a maximum deviation of  $0.002 \text{ \AA}$ ; this plane is approximately normal to that of the cyclopropane ring.  $N_2$  and M (the midpoint of the  $C_3 - C_4$  bond) are  $0.08 \text{ \AA}$  from this plane.

The  $N_1 - N_2$  bond distance of  $1.429 \text{ \AA}$  is shorter than that corresponding to the generally accepted single-bond covalent radius of  $0.74 \text{ \AA}$  for nitrogen (14). Although the difference in electronegativity between the two nitrogen atoms in cyclopropanecarbohydrazide might lead to a small shortening of the N-N bond, it is felt that the value of  $1.429 \text{ \AA}$  found in this compound presents evidence that a better value for the "normal" nitrogen-nitrogen single-bond distance is in the range of  $1.43 - 1.45 \text{ \AA}$ . Collin and Lipscomb (15) found the N-N distance in crystalline hydrazine to be  $1.46 \text{ \AA}$ .

The  $C_1 - C_2$  bond is significantly shorter than the normal single-bond distance of  $1.54 \text{ \AA}$ . It appears probable that this shortening is brought about by the conjugating power of the cyclopropane ring. In many chemical reactions the cyclopropane group tends to

behave like a double bond; in particular, when it is located near an unsaturated linkage such as a carbonyl group or an olefinic double bond, the resulting changes in dipole moments, shifts in absorption spectra, and reaction properties of the molecule can be interpreted on the basis of the conjugation between the cyclopropane ring and the unsaturated linkage. \* In Table 7 are listed some distances for carbon-carbon single bonds located between unsaturated or conjugating systems. While the analogy between most of these

Table 7

Bond lengths for carbon-carbon single bonds between conjugating systems. Standard deviations are quoted where available.

compound	d(Å)	$\sigma$ (Å)	reference
1, 3 - butadiene	1.47		Bastiansen**
diphenyl	1.48		Bastiansen (17)
benzoic acid	1.48	0.016	Sim, Robertson, and Goodwin (18)
nicotinamide	1.524	0.017	Wright and King (19)
1, 3, 5 - triphenyl- benzene	1.51, 1.48, 1.50	0.03	Farag (20)
salicylic acid	1.458	0.009	Cochran (21)
oxamide	1.542	0.006	Ayerst and Duke (22)
oxalic acid dihydrate	1.529	0.020	Ahmed and Cruickshank (23)

\*\*Private communication quoted by Allen and Sutton (24)

compounds and cyclopropanecarbohydrazide is far from complete, it is interesting to note that the magnitude of the shortening is about

\* Roberts (16) gives a list of references on this topic.

the same. Using Pauling's notation (25), a C-C distance of  $1.48 \text{ \AA}$  corresponds to about 10 - 15% double-bond character.

If the  $C_1 - C_2$  bond contains some double-bond character, one would expect that the  $C_3 C_2 C_4$  angle in the cyclopropane ring would be slightly greater than  $60^\circ$ , and that the  $C_3 - C_4$  bond distance would be the largest in the ring. The opposite effect is, in fact, observed. However, it is felt that the uncertainties in the bond lengths are such that the differences in the ring distances and angles in cyclopropanecarbohydrazide are of doubtful significance.\* The average distance of  $1.50 \text{ \AA}$  is not unreasonable; the generally accepted value for cyclopropane itself is  $1.52 \text{ \AA}$ , while in spiro-pentane (29) central distances of  $1.48 \text{ \AA}$  are reported. Similar short distances are found in Feist's acid (30). In ethylene oxide and ethylene sulfide (31), and the analogous nitrogen compound (32) one finds C-C distances of 1.47, 1.49, and  $1.48 \text{ \AA}$  respectively.

Hydrogen Bonds. The hydrogen bond distances and angles are listed in Table 8. Each oxygen atom has associated with it two hydrogen bonds -- one "strong" bond along the b axis from an  $\alpha$ -nitrogen

---

\* It has been pointed out by Professor Roberts (26) that there is evidence from solvolysis rate studies indicating that a possible stabilization of the bonded amide-cyclopropane system might result from a configuration in which the planes of the amide group and the cyclopropane ring are not normal to one another (27). The nature of this stabilization might be expected to produce asymmetry in the ring bond lengths. Although the sense of the asymmetry observed in the cyclopropane ring in cyclopropanecarbohydrazide is in agreement with these predictions, the value observed for the dihedral angle --  $89^\circ 22'$  -- is so close to  $90^\circ$  as to make any such effect of doubtful significance. On the basis of Walsh's (28) model of cyclopropane, one would predict the dihedral angle to be  $90^\circ$ .

Table 8  
Hydrogen-bond data

bond	d(Å)	∠ HN ... X (degrees)
N <sub>1</sub> H <sub>6</sub> ... O	2.94	6.7
N <sub>2</sub> H <sub>8</sub> ... N <sub>2</sub> '	3.16	10.1
N <sub>2</sub> H <sub>7</sub> ... O	3.26	19.9

and a long, weak interaction (approximately in the (010) plane) with a terminal nitrogen atom. The main bond is shown dotted in Figure 10; the long NH...O bond (and the NH...N bond) is shown dotted in Figure 11. The long N<sub>2</sub>H...O distance (3.26 Å) and the associated angle are such that the bond must be considered a very weak link.

The 3.16 Å distance for the NH...N bond in cyclopropanecarbohydrazide is a little larger than the average value of 3.11 Å found in a tabulation of NH...N distances by Robertson (33). The NH...N bonds link terminal nitrogens across the twofold screw axis, forming a zigzag chain of hydrogen bonds up the b axis. It is interesting to note that crystalline hydrazine (15) has non-bonded nitrogens related by a twofold screw axis just as in this case; in hydrazine the distance is 3.19 Å. Although no direct observation of the hydrogen positions was made in Collin and Lipscomb's determination, the conclusions at which they arrived lead to the same sort of N...N hydrogen bonding as was found in cyclopropanecarbohydrazide.

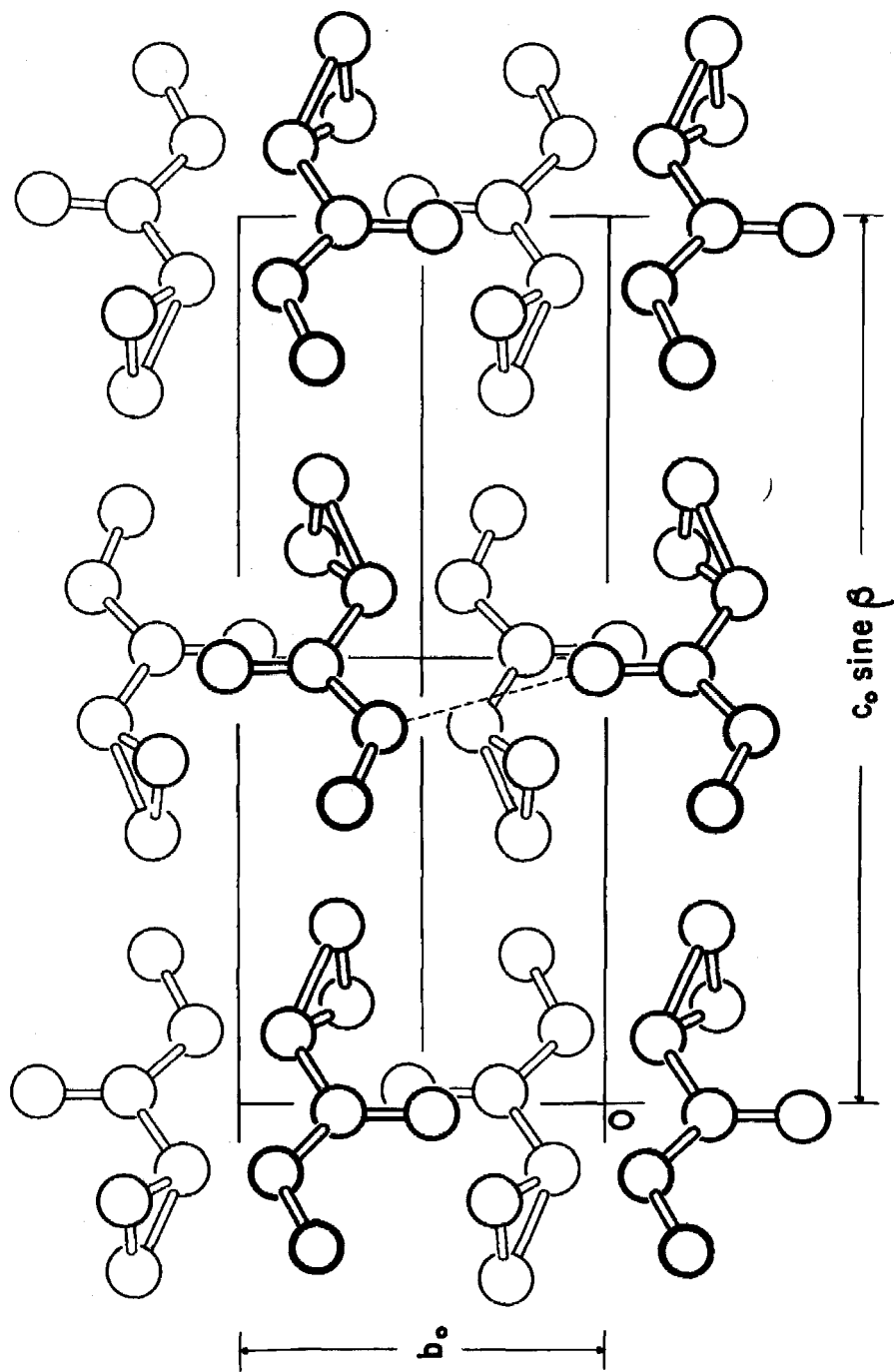


Figure 10. A view of the structure along the  $a$  axis. The dotted line shows the strong NH ... O hydrogen bond.

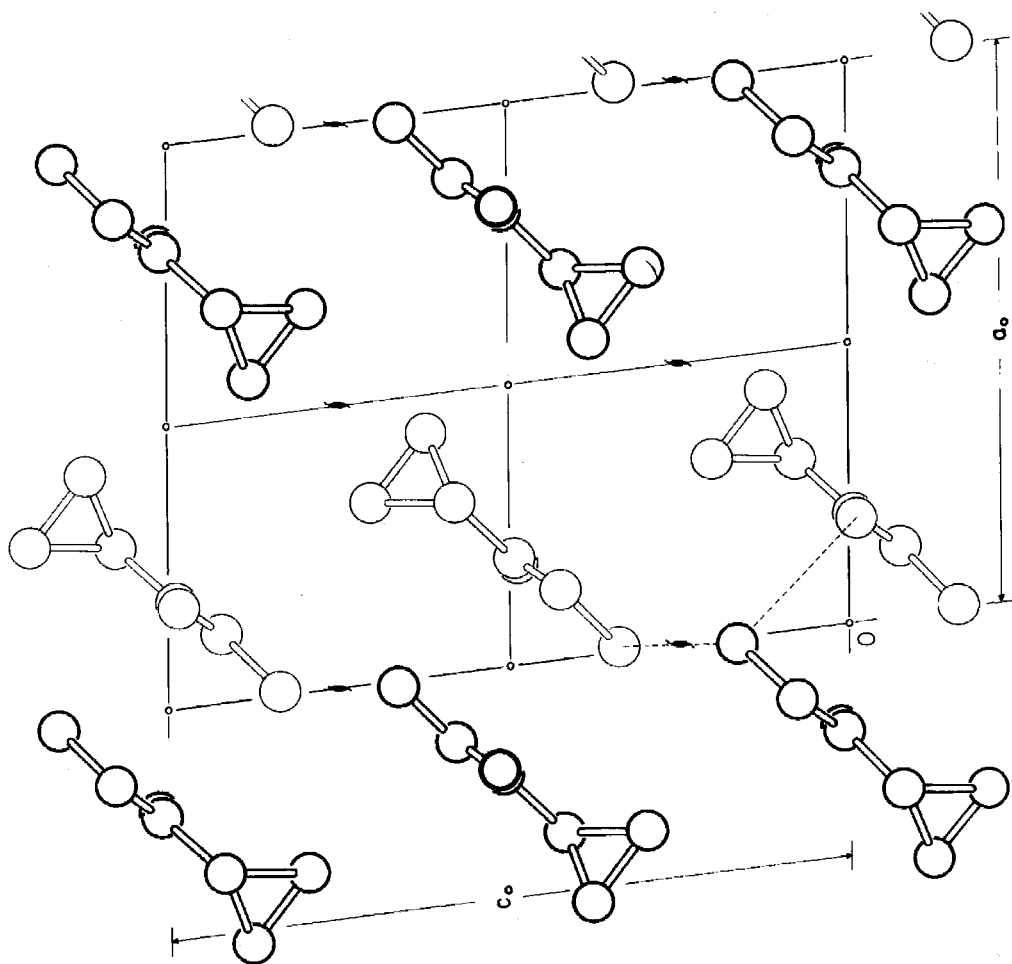


Figure 11. A view of the structure along the b axis. The dotted lines show the NH...N and the long NH...O hydrogen bonds.

Molecular Packing. Figure 11 shows that the molecules form a sheet-like structure, the sheets being oriented parallel to the  $(10\bar{1})$  plane. In view of the  $\text{NH}\cdots\text{N}$  hydrogen bonds joining the terminal nitrogen atoms, these sheets are perhaps better described as two-molecule-wide ribbons running along the  $b$  axis in the  $(10\bar{1})$  plane. Thus, the resulting atomic motions shown in Figure 8 -- which shows a remarkable degree of agreement with the type of thermal vibrations one would expect in this structure -- can be described as a superposition of a molecular motion normal to these sheets and the atomic oscillations to be expected in the "free" molecule.

Nearly all the intermolecular distances are consistent with the values predicted by Pauling's (34) Van der Waals' radii. The distances between  $\text{C}_3$  - and  $\text{C}_4$  - type atoms related by a screw axis (see Figure 11) represent the shorted non-bonding C-C distances in the structure; they are 3.92, 3.76, 3.99, and 4.23 Å, the latter two values corresponding to the  $\text{C}_3 - \text{C}'_3$  and  $\text{C}_4 - \text{C}'_4$  intermolecular contacts. That these distances are essentially equal to twice the Van der Waals' radius for an unrestricted methyl group is indicative of a rather loose packing, an effect one might expect with the relatively large thermal motion found in the crystal.

Acknowledgement. The author wishes to thank Professor J. D. Roberts for providing the crystals used in this investigation and for helpful discussions.

## APPENDIX I

Calculated and observed structure factors.  
All terms have been multiplied by 10.

$l$	$/F_{obs}/$	$F_{cal}$	$l$	$/F_{obs}/$	$F_{cal}$
	0 0 $l$			3 0 $l$	
2	433	447	-12	< 26	14
4	< 16	- 8	-10	< 35	43
6	119	92	- 8	96	- 81
8	< 24	- 19	- 6	111	- 84
10	87	68	- 4	267	-247
12	68	56	- 2	525	-598
			0	26	- 30
	1 0 $l$		2	410	-453
-12	51	59	4	181	-147
-10	62	- 60	6	63	65
- 8	122	-112	8	195	-176
- 6	119	104	10	105	-120
- 4	112	- 76			
- 2	378	317		4 0 $l$	
0	283	273	-12	< 33	26
2	36	24	-10	< 32	- 40
4	284	258	- 8	42	25
6	181	167	- 6	296	273
8	75	60	- 4	59	61
10	< 27	- 12	- 2	59	- 55
			0	< 16	8
	2 0 $l$		2	151	-135
-12	< 31	- 15	4	108	- 87
-10	67	- 45	6	< 24	- 40
- 8	< 40	57	8	< 31	23
- 6	123	- 72	10	42	- 28
- 4	588	-614			
- 2	701	-960		5 0 $l$	
0	230	-208	-10	< 27	3
2	239	178	- 8	102	80
4	227	-191	- 6	181	151
6	126	122	- 4	253	227
8	66	- 48	- 2	189	162
10	111	-102	0	98	92
			2	< 19	- 5
			4	53	- 52
			6	265	249
			8	149	134
			10	30	- 38



$l$	$/F_{\text{obs}}/$	$F_{\text{cal}}$	$l$	$/F_{\text{obs}}/$	$F_{\text{cal}}$
<i>6 0 l</i>			<i>0 1 l</i>		
-10	< 27	- 6	1	49	- 60
- 8	55	- 52	2	67	64
- 6	79	62	3	201	-203
- 4	117	97	4	26	26
- 2	54	- 50	5	262	-270
0	189	159	6	< 20	10
2	96	91	7	157	-149
4	65	70	8	90	-105
6	124	104	9	86	- 84
8	< 50	- 16	10	< 29	37
10	< 47	15	11	< 26	12
			12	< 26	19
<i>7 0 l</i>			<i>1 1 l</i>		
-10	< 40	- 31	-12	31	16
- 8	87	- 66	-11	< 31	16
- 6	49	- 42	-10	33	27
- 4	88	- 72	- 9	< 29	12
- 2	41	39	- 8	42	- 20
0	110	120	- 7	< 27	5
2	71	- 55	- 6	56	- 63
4	147	-152	- 5	58	- 51
6	66	- 60	- 4	70	- 62
			- 3	134	-128
			- 2	466	606
			- 1	33	9
			0	426	626
			1	69	90
			2	335	-431
			3	167	-189
			4	85	86
			5	166	-171
			6	< 24	8
			7	104	- 91
			8	50	- 55
			9	79	- 59
			10	85	86
<i>8 0 l</i>					
- 8	44	- 37			
- 6	39	- 29			
- 4	< 35	14			
- 2	43	- 42			
0	84	- 84			
2	61	- 60			
4	96	- 84			
<i>9 0 l</i>					
- 2	70	- 83			
0	55	63			
2	45	50			
4	< 31	- 27			
<i>10 0 l</i>					
- 2	31	37			
0	43	44			
2	29	16			

$l$	$/F_{\text{obs}}/$	$F_{\text{cal}}$	$l$	$/F_{\text{obs}}/$	$F_{\text{cal}}$
	2 1 $l$			4 1 $l$	
-11	59	45	- 9	29	- 29
-10	65	- 81	- 8	44	- 42
- 9	89	67	- 7	< 22	0
- 8	37	24	- 6	38	- 32
- 7	149	120	- 5	51	46
- 6	82	72	- 4	134	-135
- 5	121	111	- 3	< 19	17
- 4	78	- 65	- 2	84	- 78
- 3	60	- 44	- 1	22	- 24
- 2	303	339	0	60	46
- 1	39	36	1	80	- 73
0	113	-132	2	147	-154
1	139	169	3	89	- 77
2	48	- 37	4	149	159
3	201	212	5	68	55
4	172	181	6	< 22	- 18
5	214	210	7	106	104
6	57	- 53	8	149	-175
7	36	40	9	36	23
8	< 40	- 15			
9	55	- 55			
10	53	50			
	3 1 $l$			5 1 $l$	
-10	< 26	- 2	- 9	42	- 37
- 9	52	31	- 8	68	67
- 8	76	89	- 7	< 24	10
- 7	101	92	- 6	70	72
- 6	131	-138	- 5	35	33
- 5	60	45	- 4	106	-118
- 4	216	-252	- 3	93	- 93
- 3	62	- 59	- 2	89	78
- 2	46	- 39	- 1	191	-211
- 1	98	106	0	< 19	11
0	82	77	1	186	-188
1	229	315	2	73	- 64
2	42	- 36	3	128	-124
3	269	328	4	33	13
4	< 23	- 10	5	< 22	- 9
5	153	151	6	< 25	- 28
6	67	72	7	< 29	27
7	79	71			
8	84	- 80			
9	< 35	- 7			
10	< 29	- 15			

$l$	$/F_{obs}/$	$F_{cal}$	$l$	$/F_{obs}/$	$F_{cal}$
	6 1 $l$			9 1 $l$	
- 9	< 29	- 12	- 2	< 29	- 28
- 8	66	57	- 1	< 30	2
- 7	< 29	- 11	0	36	- 43
- 6	48	36	1	29	26
- 5	22	- 20			
- 4	63	60		10 1 $l$	
- 3	40	- 30			
- 2	35	43	0	39	52
- 1	< 21	- 6			
0	52	- 54		0 2 $l$	
1	55	- 47	0	205	-225
2	57	- 69	1	123	-135
3	108	-100	2	189	195
4	74	73	3	89	- 82
5	79	- 72	4	132	145
6	132	158	5	45	50
			6	76	- 60
	7 1 $l$		7	< 24	- 10
- 6	51	53	8	< 35	16
- 5	41	32	9	< 36	5
- 4	< 28	- 26	10	< 33	- 13
- 3	61	60	11	< 32	6
- 2	33	- 36	12	< 32	- 4
- 1	72	70			
0	73	75		1 2 $l$	
1	36	35	-10	30	41
2	40	2	- 9	53	- 58
3	41	- 31	- 8	31	41
4	54	59	- 7	53	- 44
5	42	- 44	- 6	99	-103
6	< 29	14	- 5	71	- 73
			- 4	23	13
	8 1 $l$		- 3	153	153
- 4	36	- 31	- 2	44	- 52
- 3	< 29	19	- 1	227	249
- 2	68	85	0	55	68
- 1	56	53	1	96	91
0	< 29	14	2	164	195
1	62	53	3	< 31	- 31
2	88	-103	4	< 38	39
3	< 33	2	5	110	-112
4	42	- 42	6	25	- 21
			7	77	- 90
			8	< 31	- 3



$l$	$/F_{\text{obs}}/$	$F_{\text{cal}}$	$l$	$/F_{\text{obs}}/$	$F_{\text{cal}}$
	<i>6 2 l</i>			<i>1 3 l</i>	
- 8	27	28	-10	41	- 45
- 7	63	68	- 9	< 33	22
- 6	< 23	- 26	- 8	88	- 88
- 5	< 23	19	- 7	< 33	- 14
- 4	< 21	1	- 6	107	-106
- 3	50	- 60	- 5	28	- 23
- 2	88	110	- 4	36	- 31
- 1	53	- 62	- 3	54	55
0	< 24	- 14	- 2	105	-101
1	53	- 55	- 1	74	- 75
2	< 21	12	0	98	-104
3	< 24	0	1	107	-106
4	< 26	6	2	17	- 17
5	60	64	3	59	59
6	< 21	- 21	4	171	-180
7	< 22	23	5	< 31	3
8	40	46	6	116	-119
			7	47	- 44
			8	< 24	- 1
			9	< 24	- 2
	<i>7 2 l</i>			<i>2 3 l</i>	
- 4	42	54	-10	< 24	27
- 3	< 23	14	- 9	< 24	1
- 2	29	17	- 8	53	- 49
- 1	26	26	- 7	27	- 22
0	< 26	- 32	- 6	68	- 75
1	< 26	- 28	- 5	< 23	3
2	< 26	22	- 4	21	- 18
3	< 26	- 15	- 3	133	130
4	36	55	- 2	79	- 70
5	30	35	- 1	72	75
			0	31	22
			1	43	32
			2	58	- 59
			3	< 21	14
			4	151	-162
			5	85	-101
			6	78	- 81
			7	37	- 45
			8	35	- 32
			9	27	43
	<i>8 2 l</i>			<i>0 3 l</i>	
- 3	27	30	1	165	-155
- 2	< 30	12	2	48	- 40
- 1	30	35	3	42	- 36
0	< 30	32	4	< 23	- 19
			5	< 20	3
			6	< 23	14
			7	< 25	21
			8	75	79
			9	38	50

$l$	$/F_{obs}/$	$F_{cal}$	$l$	$/F_{obs}/$	$F_{cal}$
	$3\ 3\ l$			$5\ 3\ l$	
-10	45	45	- 7	31	- 37
- 9	< 35	12	- 6	< 24	5
- 8	< 37	5	- 5	69	- 79
- 7	27	- 29	- 4	37	40
- 6	45	38	- 3	< 24	25
- 5	27	29	- 2	47	- 49
- 4	32	22	- 1	35	45
- 3	129	139	0	< 22	- 13
- 2	22	6	1	< 22	14
- 1	69	61	2	41	39
0	62	53	3	< 22	16
1	52	- 55	4	36	44
2	113	117	5	35	- 34
3	< 33	1	6	53	59
4	64	69	7	33	- 33
5	41	34			
6	< 45	- 44		$6\ 3\ l$	
7	< 37	15	- 4	31	- 37
8	< 35	- 16	- 3	< 25	18
9	35	42	- 2	69	- 89
			- 1	38	- 44
	$4\ 3\ l$		0	66	- 82
-10	31	32	1	51	- 60
- 9	< 28	19	2	33	- 28
- 8	44	49	3	< 26	6
- 7	< 23	8	4	< 25	- 4
- 6	< 24	10	5	< 25	4
- 5	35	- 35	6	< 24	- 18
- 4	30	24	7	28	- 35
- 3	< 22	- 9			
- 2	36	32		$7\ 3\ l$	
- 1	< 18	- 24	- 2	< 26	- 12
0	85	96	- 1	31	- 24
1	30	23	0	48	- 70
2	177	199	1	29	- 33
3	109	133	2	28	- 35
4	61	54	3	< 25	19
5	< 24	19	4	31	- 43
6	28	22			
7	31	- 43		$8\ 3\ l$	
			- 2	< 23	2

$l$	$/F_{\text{obs}}/$	$F_{\text{cal}}$	$l$	$/F_{\text{obs}}/$	$F_{\text{cal}}$
	9 3 $l$		- 5	42	29
- 2	25	32	- 4	< 42	- 14
	0 4 $l$		- 3	43	34
0	49	47	- 2	< 43	- 10
1	32	32	- 1	29	21
2	20	24	0	29	- 24
3	59	- 45	1	126	130
4	95	84	2	79	- 73
5	99	- 90	3	128	127
6	129	118	4	91	-118
7	< 26	- 3	5	< 18	14
8	60	52	6	36	- 32
9	< 24	6	7	36	25
	1 4 $l$		8	< 18	7
-11	33	35	9	33	22
-10	< 17	- 16		3 4 $l$	
- 9	31	30	- 9	23	- 14
- 8	< 18	- 8	- 8	48	- 42
- 7	23	17	- 7	71	- 61
- 6	< 38	30	- 6	21	- 14
- 5	101	93	- 5	< 46	- 47
- 4	< 33	5	- 4	< 37	- 4
- 3	90	95	- 3	50	- 35
- 2	33	23	- 2	38	- 24
- 1	64	79	- 1	53	- 35
0	< 23	4	0	< 41	- 38
1	96	106	1	< 47	39
2	< 29	14	2	130	-124
3	57	43	3	43	- 28
4	64	58	4	106	-105
5	42	28	5	67	- 68
6	63	58	6	41	- 31
7	67	65	7	20	15
8	48	39	8	25	- 18
9	35	32	9	< 14	16
	2 4 $l$			4 4 $l$	
-11	17	19	- 9	18	- 15
-10	49	- 46	- 8	17	8
- 9	< 35	- 7	- 7	46	- 40
- 8	58	- 54	- 6	< 18	10
- 7	21	- 17	- 5	< 18	- 4
- 6	54	- 49	- 4	35	- 26
			- 3	59	- 55
			- 2	< 16	4

$l$	$/F_{\text{obs}}/$	$F_{\text{cal}}$	$l$	$/F_{\text{obs}}/$	$F_{\text{cal}}$
- 1	119	-127	6	32	33
0	51	38	7	31	22
1	81	- 78			
2	41	30		7 4 $l$	
3	38	- 36			
4	◁ 17	1	- 6	◁ 14	9
5	43	- 38	- 5	35	42
6	42	- 33	- 4	34	- 37
7	33	- 20	- 3	◁ 20	23
8	33	- 26	- 2	50	- 49
9	23	- 18	- 1	◁ 18	- 2
			0	29	- 31
	5 4 $l$		1	26	29
- 9	◁ 17	19	2	◁ 17	- 6
- 8	◁ 16	13	3	33	31
- 7	◁ 20	14	4	25	18
- 6	◁ 18	- 8	5	◁ 16	5
- 5	◁ 18	- 1	6	19	19
- 4	◁ 17	8			
- 3	33	- 37		8 4 $l$	
- 2	55	54	- 6	◁ 13	- 9
- 1	54	- 52	- 5	◁ 14	- 12
0	94	100	- 4	◁ 16	- 14
1	23	15	- 3	◁ 14	1
2	92	89	- 2	27	- 28
3	27	16	- 1	◁ 18	- 11
4	◁ 18	13	0	26	- 27
5	50	- 48	1	◁ 14	- 11
6	◁ 17	5	2	◁ 14	- 10
7	18	- 13	3	◁ 14	1
			4	◁ 14	- 13
	6 4 $l$				
- 9	14	15		9 4 $l$	
- 8	◁ 14	- 1	- 1	19	- 28
- 7	◁ 16	- 1	0	◁ 13	1
- 6	◁ 17	15	1	◁ 11	- 4
- 5	38	37			
- 4	◁ 18	13			
- 3	51	61		0 5 $l$	
- 2	◁ 18	- 5	1	106	- 92
- 1	◁ 21	18	2	◁ 25	- 7
0	29	29	3	76	- 71
1	39	31	4	◁ 23	- 12
2	33	25			
3	29	25			
4	26	28			
5	◁ 16	5			



$l$	$/F_{\text{obs}}/$	$F_{\text{cal}}$	$l$	$/F_{\text{obs}}/$	$F_{\text{cal}}$
	1 5 $l$			3 5 $l$	
- 5	38	30	- 5	37	34
- 4	◁ 38	- 23	- 4	36	28
- 3	◁ 35	- 25	- 3	37	30
- 2	66	- 56	- 2	37	29
- 1	◁ 31	- 15	- 1	79	72
0	64	- 52	0	◁ 33	11
1	◁ 31	30	1	80	81
2	35	- 33	2	◁ 31	- 14
3	90	- 85	3	◁ 30	18
4	◁ 25	14	4	38	- 33
	2 5 $l$			0 6 $l$	
- 5	77	67	0	◁ 16	10
- 4	◁ 36	- 32			
- 3	68	61			
- 2	◁ 38	- 21			
- 1	84	75			
0	◁ 38	- 18			
1	◁ 38	24			
2	◁ 37	0			
3	◁ 36	- 24			
4	◁ 26	- 1			

## APPENDIX II

Geometric structure factors and formulae for  
space group  $P2_1/c - C_{2h}^5$

origin at  $\bar{1}$

b as unique axis

equivalent positions:  $\pm / x, y, z$  ;  $x, 1/2 - y, 1/2 + z /$

$$F(hkl) = \sum_j^{N/4} f_j A_j + i \sum_j^{N/4} f_j B_j$$

general:

$$A_j = 4 \cos 2\pi (hx_j + lz_j + \frac{k+l}{4}) \cos 2\pi (ky_j - \frac{k+l}{4})$$

$$B_j = 0$$

$$A = B = 0 \text{ if } h = l = 0 \text{ or if } k = 0$$

$k + l = 2n$ :

$$A_j = 4 \cos 2\pi (hx_j + lz_j) \cos 2\pi ky_j ; B_j = 0$$

$$F(hkl) = +F(h\bar{k}l) \neq F(\bar{h}kl) ; F(\bar{h}kl) = F(hk\bar{l})$$

$k + l = 2n + 1$ :

$$A_j = -4 \sin 2\pi (hx_j + lz_j) \sin 2\pi ky_j ; B_j = 0$$

$$F(hkl) = -F(h\bar{k}l) \neq F(\bar{h}kl) ; F(\bar{h}kl) = -F(hk\bar{l})$$

electron density:

$$\rho(XYZ) = 4/V \left\{ \begin{aligned} & \sum_h^{k+l=2n} \sum_k \sum_l [F(hkl) \cos 2\pi (hX + lZ) \\ & + F(\bar{h}kl) \cos 2\pi (-hX + lZ)] \cos 2\pi kY \\ & - \sum_h^{k+l=2n+1} \sum_k \sum_l [F(hkl) \sin 2\pi (hX + lZ) \\ & + F(\bar{h}kl) \sin 2\pi (-hX + lZ)] \sin 2\pi kY \end{aligned} \right\}$$

## REFERENCES TO PART I

1. J. D. Roberts, J. Amer. Chem. Soc. 73, 2959 (1951).
2. R. A. Pasternak, Acta Cryst. 9, 341-349 (1956).
3. D. Harker, J. S. Kasper, Acta Cryst. 1, 70-75 (1948).
4. L. H. Jensen, E. C. Lingafelter, Acta Cryst. 6, 300-301 (1953).
5. J. A. Hoerni, J. A. Ibers, Acta Cryst. 7, 744-746 (1954).
6. R. McWeeny, Acta Cryst. 4, 513-519 (1951).
7. J. Berghius, IJ. M. Haanappel, M. Potters, B. O. Loopstra, A. L. Veenendaal, C. H. MacGillivray, Acta Cryst. 8, 478-483 (1955).
8. E. W. Hughes, J. Amer. Chem. Soc. 63, 1737-1752 (1941).
9. D. R. Davies, J. J. Blum, Acta Cryst. 8, 129-136 (1955).
10. W. Cochran, Acta Cryst. 4, 408-411 (1951).
11. J. Waser, Acta Cryst. 8, 731 (1955).
12. D. W. J. Cruickshank, Acta Cryst. 9, 757-758 (1956).
13. L. Pauling, R. B. Corey, Proc. Royal Soc. B, 141, 10-20 (1953).
14. V. Schomaker, D. P. Stevenson, J. Amer. Chem. Soc. 63, 37-40 (1941).
15. R. L. Collin, W. N. Lipscomb, Acta Cryst. 4, 10-14 (1951).
16. J. D. Roberts, R. H. Mazur, J. Amer. Chem. Soc. 73, 2509-2520 (1951).
17. O. Bastiansen, Acta Chem. Scand. 3, 408-414 (1949).
18. G. A. Sim, J. M. Robertson, T. H. Goodwin, Acta Cryst. 8, 157-164 (1955).
19. W. B. Wright, G. S. D. King, Acta Cryst. 7, 283-288 (1954).
20. M. S. Farag, Acta Cryst. 7, 117-121 (1954).
21. W. Cochran, Acta Cryst. 6, 260-268 (1953).
22. E. M. Ayerst, J. R. C. Duke, Acta Cryst. 7, 588-590 (1954).

23. F. R. Ahmed, D. W. J. Cruickshank, Acta Cryst. 6, 385-392 (1953).
24. P. W. Allen, L. E. Sutton, Acta Cryst. 3, 46-72 (1950).
25. L. Pauling, The Nature of the Chemical Bond, Cornell Univ. Press, 1948, pg. 175.
26. J. D. Roberts, private communication, April, 1957.
27. J. D. Roberts, W. Bennett, R. Armstrong, J. Amer. Chem. Soc. 72, 3329-3333 (1950).
28. A. D. Walsh, Trans. Faraday Soc. 45, 179-190 (1949).
29. J. Donohue, G. L. Humphrey, V. Schomaker, J. Amer. Chem. Soc. 67, 332-335 (1945).
30. D. R. Peterson, Chemistry and Industry, 904-905 (1956).
31. G. L. Cunningham, Jr., A. W. Boyd, R. J. Myers, W. D. Gwinn, W. I. Le Van, J. Chem. Phys. 19, 676-685 (1951).
32. T. E. Turner, V. C. Fiora, W. M. Kendrick, J. Chem. Phys. 23, 1966 (1955).
33. J. M. Robertson, Organic Crystals and Molecules, Cornell Univ. Press, 1953, pp. 243-245.
34. L. Pauling, The Nature of the Chemical Bond, Cornell Univ. Press, 1948, pg. 189.

II.

A THEORY OF ISOTROPIC HYPERFINE INTERACTIONS

IN  $\pi$ -ELECTRON RADICALS

## INTRODUCTION

This investigation presents further consideration of the relation between the molecular electronic structure of  $\pi$ -electron radicals and the isotropic proton hyperfine splittings which are observed in the electron magnetic resonance spectra of these radicals in liquid solutions (1). By  $\pi$ -electron radicals one refers especially to the positive, neutral, and negative ion radicals of planar aromatic hydrocarbons where, to a first approximation, the unpaired electron(s) moves in a  $\pi$ -molecular orbital antisymmetric with respect to the molecular plane. The hyperfine splittings of interest are those arising from in plane aromatic protons which have now been observed in numerous aromatic molecular radicals (1). As has been pointed out by McConnell (2, 3), Bersohn (4), Weissman (5), and Fraenkel and Venkataraman (6), the observed proton hyperfine splittings can result from  $\sigma$ - $\pi$  electron exchange interaction. In fact, it has been suggested (1, 2, 3) that the nature of this  $\sigma$ - $\pi$  electron exchange interaction is such that the proton hyperfine splitting can be used to measure unpaired electron distributions on the carbon atoms. In particular, it was proposed that if  $a_N$  is the hyperfine splitting due to aromatic proton N, then  $a_N$  is related to the "unpaired electron density" at carbon atom N,  $\rho_N$ , by the simple equation

$$a_N = Q \rho_N \quad (1)$$

Here  $Q$  is a semi-empirical constant,  $Q \approx -30 \pm 5$  gauss, or  $-85 \pm 15$  Mc;  $Q$  is assumed to be the same for all aromatic CH bonds in all molecular systems.

A recent review of experimental and theoretical work bearing on equation 1 is given elsewhere (1). The principal purpose in undertaking the present work has been to examine from a critical point of view the qualitative and semi-quantitative validity of equation 1. The principal conclusion that is reached is that equation 1 retains its validity even when weak  $\pi$ - $\pi$  configuration interaction is included in the calculations, provided  $\rho_N$  is generalized to be the expectation value of a spin density operator,  $\underline{\rho}_N$ . In this case  $\rho_N$  can be positive or negative, and the  $a_N$  are then negative or positive, respectively. The quantity  $\rho_N$  is the "spin density at carbon atom N." A preliminary account of this aspect of the present work has been published (7).

Brovetto and Ferroni (8) implicitly assumed a relation similar to equation 1 in their interpretation of the proton hyperfine splittings in the triphenylmethyl radical using the valence bond approximation for the unpaired electron distribution. These workers apparently did not recognize the indirect character of the  $\pi$ -electron-proton hyperfine interactions.

### THE CONTACT HYPERFINE HAMILTONIAN

For large applied fields (Paschen-Back region), one need only consider the hyperfine interaction between the z-components of the electron and nuclear spins; in this approximation the Fermi contact Hamiltonian (9) which gives the isotropic non-vanishing hyperfine splitting for molecules in solution (2, 9) is

$$H_N = \left( \frac{8\pi g |\beta|}{3} \right) \left( \frac{u_I}{I} \right) \sum_k \delta(\underline{r}_{kN}) S_{kz} I_{Nz} \quad (2)$$

where  $|\beta|$  is the absolute magnitude of the Bohr magneton,  $\delta(\underline{r}_{kN})$  is the Dirac delta function of the distance  $\underline{r}_{kN}$  between electron  $k$  and nucleus  $N$ ,  $u_I$  is the magnetic moment of proton  $N$ , and  $I_{Nz}$  is the  $z$ -component of the spin of proton  $N$ , in units of  $\hbar$ . Equation 2 can also be expressed in terms of the "coupling constant" for proton  $N$ ,  $a_N$ ,

$$H_N = h a_N S_z I_{Nz} \quad (3)$$

where  $S_z$  is the total  $z$ -component of the electron spin angular momentum. Thus, if  $\Psi$  is the ground state electronic wave function,

$$a_N = \left( \frac{8\pi g |\beta|}{3h} \right) \left( \frac{u_I}{I} \right) \delta_N \quad (4)$$

$$\delta_N = \frac{1}{S_z} \langle \Psi | \sum_k \delta(\underline{r}_{kN}) S_{kz} | \Psi \rangle \quad (5)$$

We seek to study the relation between  $a_N$  and the unpaired electron distribution.

Absolute values of  $a_N$ ,  $|a_N|$ , are easily deduced from hyperfine splittings in high field electron magnetic resonance spectra. The signs of the  $a_N$ 's are considerably more difficult to determine experimentally but are of considerable theoretical importance as



will be shown later. The signs of the  $a_N$ 's can in principle be determined if the nuclear resonances of protons N can be observed, and if shifts in these resonances are sufficiently large and are dominated by the contact hyperfine interaction.

Consider a system characterized by a paramagnetic relaxation time  $T_1$ , or an exchange time  $T_e$  such that  $T_1^{-1}$  or  $T_e^{-1} \gg a_N$ ; then proton N will see a single average hyperfine magnetic field corresponding to the effective spin Hamiltonian for proton N

$$H = -u_{Nz} \left( H_0 - 2\pi a_N \left( \frac{I\hbar}{u_I} \right) \langle S_z \rangle \right) \quad (6)$$

where  $\langle S_z \rangle$  is the time average value of the z-component of the electron spin. For a system obeying the Curie Law,

$$\langle S_z \rangle = \frac{-g|\beta|S(S+1)}{3kT} H_0 \quad (7)$$

so that

$$H = -u_{Nz} \left( 1 + 2\pi a_N \left( \frac{I\hbar}{u_I} \right) \frac{g|\beta|S(S+1)}{3kT} \right) H_0 \quad (8)$$

Since  $u_I$  is positive for the proton it is seen that when the proton resonance of N is observed at a fixed frequency, the contact shift will be to lower applied fields when  $a_N$  is positive, and to higher applied fields when  $a_N$  is negative. In substances with unpaired electrons in open-shell s-orbitals the electron spin and nuclear

spin interaction is direct, the quantity corresponding to  $\delta_N$  in equation 5 is positive, and  $a_N$  has the sign of  $u_I$ . In such cases  $a_N/u_I$  is always positive and the second term in parentheses in equation 8 is positive. Thus, "normal" nuclear paramagnetic shifts are to lower fields. As will be seen, a characteristic feature of the calculated  $a_N$ 's in aromatic radicals is that they are most often, but not always, negative; the predicted proton shifts are to higher applied fields at constant applied radio frequency.\*

### $\sigma$ - $\pi$ ELECTRON INTERACTION IN A CH FRAGMENT

To begin the treatment of hyperfine splittings in planar aromatic radicals it is convenient to consider a hypothetical CH fragment which is abstracted from an aromatic radical. One considers the  $\sigma$ - $\pi$  electron interaction between the two  $\sigma$ -bonding electrons and the single unpaired  $\pi$ -electron which is considered to be in a pure  $2p_z$  atomic orbital. The occurrence of unpaired spin density at the proton can be understood qualitatively in terms of the following approximate treatments of molecular electronic structure: (a) the valence bond model

---

\* It has been pointed out by Dr. McConnell (10) that the above conditions on the validity of equations 6 and 8 for the nuclear resonance shift with regard to the relative value of  $a_N$  and  $T_I^{-1}$  or  $T_e^{-1}$  imply the absence of observable hyperfine splittings in the same system for which equations 6 and 8 are valid. That is, if  $T_e^{-1} \gg a_N$  the hyperfine splittings are obscured by exchange narrowing, and if  $T_I^{-1} \gg a_N$  the paramagnetic line widths are greater than the splittings. This is clearly a convenient experimental criterion for the observability of contact nuclear resonance shifts.

with a single orbital configuration, and (b) a molecular orbital model with  $\sigma$ - $\pi$  configuration interaction.\* The basic ingredients of these two treatments in their application to the three-electron problem of the CH fragment are summarized below.

(a). Valence Bond Approximation. McConnell (2) has applied simplified valence bond theory to the CH fragment, and Jarrett (11) has proposed quantitative improvements on these calculations. Bersohn (4) has carried out a rather elaborate calculation of  $\sigma$ - $\pi$  electron interactions in planar  $C_2H_4^+$  using integrals obtained by Altman (12) in his work on ethylene. The basic ingredients of the valence bond approximation are summarized here in its application to this problem, and, in particular, reference is made to the theoretically deduced sign of the hyperfine coupling.

Let  $h$  denote an  $sp^2$  hybrid orbital centered on the carbon atom and directed toward the proton;  $p$  is a  $2p_z$  atomic orbital centered on the carbon atom and is used in building up the  $\pi$ -molecular orbitals for the complete  $\pi$ -electron system. The hydrogen atom  $1s$  orbital,  $s$ , is centered on the proton in the CH fragment. A simple covalent CH bond is represented by the normalized doublet state eigenfunction,

$$\phi_1^0 = A \frac{1}{\sqrt{2}} \frac{1}{\sqrt{1+S_0^2}} p h s \{ \alpha \alpha \beta - \alpha \beta \alpha \} \quad (9)$$

---

\* A similar treatment for the "unrestricted" Hartree-Fock method is given elsewhere (10).

Here  $A$  is the antisymmetrization and renormalization operator and  $S_0$  is the h-s overlap integral:

$$S_0 = \langle h/s \rangle \quad (10)$$

An excited doublet state of the same electron configuration which corresponds to antibonding between the carbon and hydrogen atoms is:<sup>\*</sup>

$$\phi_2^0 = A \frac{1}{\sqrt{6}} \frac{1}{\sqrt{1 - S_0^2}} \text{phs} \left\{ \alpha\alpha\beta + \alpha\beta\alpha - 2\beta\alpha\alpha \right\} \quad (11)$$

$H$  denotes the three-electron Hamiltonian for the electronic kinetic energy and electrostatic potential energy, including nuclear attraction terms. As has been shown previously (2), the "first-order" mixing of  $\phi_2^0$  with  $\phi_1^0$  gives for the ground state wave function,

$$\phi_1 = \phi_1^0 + \lambda \phi_2^0 \quad (12)$$

where it is assumed that  $|\lambda|^2 \ll 1$ , and where

$$\lambda = - \frac{H_{21}}{\Delta E_{21}} \quad (13)$$

$$\Delta E_{21} = H_{22} - H_{11} \quad (14)$$

$$H_{ij} = \langle \phi_i | H | \phi_j \rangle \quad (15)$$

\* In the three-electron functions  $\phi_1^0$  and  $\phi_2^0$  and in the polyelectron functions considered later, the labels for the electron coordinates always appear in serial order. For example,

$$\text{phs } \alpha\alpha\beta = p(1) h(2) s(3) \alpha(1) \alpha(2) \beta(3)$$

$$H_{21} = - \frac{\sqrt{3}}{2} \frac{1}{\sqrt{1 - S_o^4}} (J_{ph} - J_{ps}) \quad (16)$$

$$J_{ph} = \langle ph \mid \frac{e^2}{r} \mid hp \rangle \quad (17)$$

$$J_{ps} = \langle ps \mid \frac{e^2}{r} \mid sp \rangle \quad (18)$$

The exchange integral given in equation 17, for example, is

$\langle p(1) h(2) \mid \frac{e^2}{r_{12}} \mid h(1) p(2) \rangle$  where  $r = r_{12}$  is the interelectronic distance.

From equations 5 and 12 one obtains  $\delta$  for the CH fragment:

$$\delta_{CH} = - \frac{2}{\sqrt{3}} \lambda \frac{1}{\sqrt{1 - S_o^4}} |s(0)|^2 \quad (19)$$

Let  $(a_{CH}^o)_{VB}$  denote the theoretically calculated valence bond hyperfine coupling constant for the CH fragment, and let  $a_H^o$  denote the hyperfine coupling constant in the hydrogen atom.

$$(a_{CH}^o)_{VB} = \frac{-1}{1 - S_o^4} \frac{J_{ph} - J_{ps}}{\Delta E_{21}} a_H^o \quad (20)$$

$$a_H^o = \frac{8\pi g |\beta|}{3h} \left( \frac{u_I}{I} \right) |s(0)|^2 = 1420 \text{ Mc} \quad (21)$$

McConnell (2) has estimated a safe order-of-magnitude energy difference between the two states  $\phi_1^o$  and  $\phi_2^o$  to be  $\Delta E_{21} = 5 - 15$  e.v. Altman (12) gives  $J_{ph} = 1.81$  e.v.,  $J_{ps} = 0.745$  e.v.;  $J_{ph}$  was previously

estimated (2) to be 1.17 e. v. from the work of Voge (13). In any event,  $(J_{ph} - J_{ps}) / \Delta E_{21}$  is positive and of the order of 0.1 - 0.01. Assuming Jarrett's value for the overlap,  $S_o \approx 0.8$ , one obtains an estimate of  $a_{CH}^o \approx 25 - 250$  Mc, which is in good order-of-magnitude agreement with the "best" semi-empirical value for  $Q$ ,  $|Q| \approx 85 \pm 15$  Mc.

(b). Molecular Orbital Theory. Weissman (5) has used molecular orbital theory for the  $\sigma$ -electrons in a discussion of aromatic proton hyperfine splittings. In this section this theory is developed further with particular reference to the CH fragment, and to the sign of the hyperfine coupling constant.

As a first approximation to the configuration interaction problem for the CH fragment one takes for the lowest energy configuration

$$\psi_1^o = A \sigma \sigma p \alpha \beta \alpha \quad (22)$$

where the  $\sigma$  bonding orbital is a linear combination of the atomic and hybrid orbitals, s and h:

$$\sigma = \frac{1}{\sqrt{2(1+S_o)}} (s + h) \quad (23)$$

Here, for simplicity, equal proportions of s and h have been assumed. That is, ionic character or charge transfer (other than the overlap effect) has been neglected.  $\psi_1^o$  gives no proton hyperfine splitting, but admixture of the doublet state excited configuration  $\psi_2^o$  does.

$$\Psi_2^0 = \frac{1}{\sqrt{6}} A \sigma \sigma^* p \left\{ 2 a a \beta - a \beta a - \beta a a \right\} \quad (24)$$

Here  $\sigma^*$  is the normalized antibonding orbital orthogonal to  $\sigma$  :

$$\sigma^* = \frac{1}{\sqrt{2(1 - S_0)}} (s - h) \quad (25)$$

A second excited doublet state with the same configuration is

$$\Psi_3^0 = \frac{1}{\sqrt{2}} A \sigma \sigma^* p \left\{ a \beta a - \beta a a \right\} \quad (26)$$

The doublet state functions  $\Psi_1^0$ ,  $\Psi_2^0$ , and  $\Psi_3^0$  are taken as the basis of a variational calculation for the mixing of  $\Psi_2^0$  and  $\Psi_3^0$  with  $\Psi_1^0$ .

The variational parameters  $\eta_2$  and  $\eta_3$  describing this mixing are assumed to be small:  $\eta_2^2 \ll 1$ ,  $\eta_3^2 \ll 1$ .

$$\Psi_1 = \Psi_1^0 + \eta_2 \Psi_2^0 + \eta_3 \Psi_3^0 \quad (27)$$

$$\eta_2 = -\frac{H_{21}}{\Delta E_{21}} ; \quad \eta_3 = -\frac{H_{31}}{\Delta E_{31}} \quad (28)$$

Here, as before,  $\Delta E_{21} = H_{22} - H_{11}$ . The mixing of  $\Psi_3^0$  with  $\Psi_1^0$  does not affect the hyperfine splitting as long as  $\eta_3$  is small.

Corresponding to equation 15 one has

$$H_{21} = -\frac{3}{\sqrt{6}} J \quad (29)$$

$$J = \left\langle \sigma^* p \left| \frac{e^2}{r} \right| p \sigma \right\rangle \quad (30)$$

$$J = \frac{1}{2} \frac{1}{\sqrt{1 - S_0^2}} (J_{ps} - J_{ph}) \quad (31)$$

From equations 5 and 27

$$\delta_{CH} = \frac{4}{\sqrt{6}} \eta_2 \sigma(0) \sigma^*(0) = \frac{2}{\sqrt{6}} \eta_2 \frac{1}{\sqrt{1 - S_0^2}} |s(0)|^2 \quad (32)$$

assuming  $|h(0)| \ll |s(0)|$ , or

$$\delta_{CH} = \frac{1}{2} \frac{1}{1 - S_0^2} \frac{J_{ps} - J_{ph}}{\Delta E_{21}} |s(0)|^2 \quad (33)$$

or,

$$(a_{CH}^o)_{MO} = - \frac{1}{2} \frac{1}{1 - S_0^2} \frac{J_{ph} - J_{ps}}{\Delta E_{21}} a_H^o \quad (34)$$

From a comparison of equations 20 and 34 it is clear that the valence bond and molecular orbital methods, in the approximations used, lead to almost identical results.

## UNPAIRED ELECTRON DISTRIBUTION AND HYPERFINE SPLITTINGS

The observed hyperfine splittings give a direct measure of the unpaired electron densities at the positions of the aromatic protons. Since the unpaired electrons are primarily localized on the carbon atoms of the aromatic ring system, it is of interest to inquire as to whether or not the observed hyperfine splitting may give information regarding the unpaired electron distribution among the carbon atoms, as has been previously



proposed (1, 2, 3). The concept of the "unpaired electron density at carbon atom N,  $\rho_N$ ," has been introduced previously. This was essentially the probability of finding an unpaired electron in a  $p_z - \pi$  atomic orbital centered on carbon atom N, and  $0 \leq \rho_N \leq 1$  for, say, an aromatic radical having one unpaired electron. This concept of unpaired electron density is only good in the one-electron approximation. In the present work one must consider  $\pi - \pi$  electron configuration interaction, and must introduce a more general expression of unpaired electron distribution. This is given by the spin density operator for carbon atom N,  $\rho_N$ , which is defined by the operator equation

$$\rho_N \sum_k S_{kz} = \sum_k \Delta_N(k) S_{kz} \quad (35)$$

Here  $\Delta_N(k)$  is a previously introduced (14) "atomic orbital delta function" which is essentially a three dimensional step function such that  $\Delta_N(k) = 1$  when electron  $k$  is in a  $p_z$  atomic orbital on carbon atom N, and  $\Delta_N(k) = 0$  elsewhere. In the present approximation, neglect of  $\pi - \pi$  overlap implies that

$$\langle p_{Nz}(k) | \Delta_{N'}(k) | p_{N''z}(k) \rangle = \delta_{NN'} \delta_{N'N''} \quad (36)$$

As shown later, expectation values of  $\rho_N$  can sometimes be negative, meaning that the unpaired spin density at carbon atom N has a polarization which is opposite to the total spin polarization of the molecule. To within the limits of the neglect of  $\pi$ -orbital overlap,

$$\sum_N \rho_N = 2S \quad (37)$$

where  $S$  is the total electron spin of the molecule,  $S = 1/2, 1, 3/2,$  etc.

The present task is to show the conditions under which there exists a simple proportionality between  $\rho_N$  and the hyperfine splitting due to proton  $N$ ,  $a_N$ . Molecular orbital theory will be used to describe the  $\pi$ -electron wave functions and, for uniformity, the  $\sigma$  CH bonds; essentially the same results would be obtained if valence bond theory were used for the  $\sigma$  CH bonds. In analogy with equation 23 let  $\sigma_N$  denote the localized CH  $\sigma$ -bonding orbital for CH bond  $N$ ;  $p_N$  denotes the corresponding  $2p_z$ - $\pi$  atomic orbital situated on carbon atom  $N$ . The lowest energy configurational function for the entire molecule is, assuming no ground state degeneracy,

$$\Psi_1^0 = A \left\{ \prod_{N=1}^M \sigma_N \sigma_N^{\alpha\beta} \right\} \left\{ \prod_{u=1}^{\lambda-1} \pi_u \pi_u^{\alpha\beta} \right\} \pi_\lambda^\alpha \quad (38)$$

Here  $\pi_u$  refers to the  $u^{\text{th}}$  doubly filled  $\pi$ -MO;  $\pi_\lambda$  is by definition the orbital which holds the unpaired electron in the ground state configuration.  $M$  denotes the number of aromatic CH bonds. The  $\pi$ -orbitals are all expressed as linear combinations of  $2p_z$  carbon atom orbitals,

$$\pi_u = \sum_N a_{Nu} p_N \quad (39)$$

In equation 38, the carbon-carbon  $\sigma$ -bonding orbitals, as well as inner shell electrons, have not been included explicitly. First order  $\sigma$ - $\pi$  configuration interaction involving these electrons does not

affect the calculated hyperfine splittings. Corresponding to the two doublet states  $\psi_2^{\circ}$  and  $\psi_3^{\circ}$  of the CH fragment, there are now  $2M$  similar zero order excited state functions:  $\psi_{21}^{\circ}, \psi_{22}^{\circ}, \dots, \psi_{2N}^{\circ}, \dots, \psi_{2M}^{\circ}; \psi_{31}^{\circ}, \psi_{32}^{\circ}, \dots, \psi_{3N}^{\circ}, \dots, \psi_{3M}^{\circ}$ .

For the purpose of the present discussion it is assumed that equation 38 represents the best possible single product eigenfunction that can be constructed using linear combinations of atomic orbitals. The functions  $\psi_i^{\circ}$  constitute a complete set, are orthonormal, and are approximate eigenfunctions of the complete exact Hamiltonian,  $H$ . Accordingly it is assumed that the non-diagonal elements of the  $H$  matrix, especially the  $H_{1k}$ , are small. The mixing of the excited configurations with the ground state configuration  $\psi_1^{\circ}$  is to be calculated using the variational method for minimizing the ground state energy. This calculation can be carried out in a manner analogous to ordinary perturbation theory, providing the  $H_{jk}$  are sufficiently small, which we assume to be the case. It is from this analogy between perturbation theory and the variational method for small  $H_{jk}$  that the terminologies "zero, first, and second order functions", and "zero, first, and second order matrix elements" are derived. The ground state function with admixture of CH  $\sigma$  configurationally excited states is then

$$\Psi_1 = \psi_1^{\circ} + \sum_N \eta_{2N} \psi_{2N}^{\circ} + \sum_N \eta_{3N} \psi_{3N}^{\circ} + \dots \quad (40)$$

The coefficients  $\eta_{2N}$  and  $\eta_{3N}$  are similar to  $\eta_2$  and  $\eta_3$  considered previously for the CH fragment. The calculation of  $a_N$  now closely

parallels the development in equations 27 - 34 for the CH fragment except for certain details. Here both first and second order contributions to  $\eta_{2n}$  are considered:

$$\eta_{2N} = \eta_{2N}^{(1)} + \eta_{2N}^{(2)} \quad (41)$$

In equation 41,  $\eta_{2N}^{(1)}$  arises from first order  $\sigma$ - $\pi$  configuration interaction as considered previously for the CH fragment;  $\eta_{2N}^{(2)}$  is a second order term arising from ground state mixing with doubly excited configurations involving both  $\sigma$  and  $\pi$ -electrons. As before,  $\psi_{3N}^0$  contributes nothing to the hyperfine splitting and is not considered further, at least in first order. Corresponding to equation 28 one has here

$$\eta_{2N}^{(1)} = - \frac{H_{2N,1}}{\Delta E_{2N,1}} \quad (42)$$

$$H_{2N,1} = \langle \psi_{2N}^0 | H | \psi_1^0 \rangle \quad (43)$$

$$= - \frac{3}{\sqrt{6}} \langle \sigma_N^* \pi_\lambda | \frac{e^2}{r} | \pi_\lambda \sigma_N \rangle \quad (44)$$

$$= - \frac{3}{\sqrt{6}} \sum_{N', N''} a_{N'\lambda} a_{N''\lambda}$$

$$\langle \sigma_N^* p_{N'} | \frac{e^2}{r} | p_{N''} \sigma_N \rangle \quad (45)$$

Since  $\sigma_N$  and  $\sigma_N^*$  are localized in the region of the CH bond, the product  $\sigma_N^* \sigma_N \frac{e^2}{r}$  is small everywhere except in the region of the

proton N and carbon atom N ; therefore all the matrix elements in equation 45 should be negligible except those for which  $N' = N'' = N$  . Therefore, equation 45 is simplified to give

$$H_{2N, 1} = - \frac{3}{\sqrt{6}} a_{N\lambda}^2 J_N \quad (46)$$

$$J_N = \langle \sigma_N^* p_N \left| \frac{e^2}{r} \right| p_N \sigma_N \rangle \quad (47)$$

By analogy with equation 30,

$$J_N = J \text{ for all } N \quad (48)$$

Corresponding to equation 32 one has here

$$\delta_N^{(1)} = \frac{2}{\sqrt{6}} \frac{\eta_{2N}^{(1)}}{\sqrt{1 - S_0^2}} |s(0)|^2 \quad (49)$$

Thus,

$$a_N^{(1)} = \rho_N^{(0)} (a_{CH}^o)_{MO} \quad (50)$$

where

$$\rho_N^{(0)} = a_{N\lambda}^2 \quad (51)$$

since the zero order spin density is defined by the equation

$$\rho_N^{(0)} = \langle \Psi_1^o | p_N | \Psi_1^o \rangle \quad (52)$$

In obtaining equation 50 it has been assumed, of course, that  $\Delta E_{2N, 1} = \Delta E_{2, 1}$  for all N. Equation 50, with  $(a_{CH}^0)_{MO} = Q$ , expresses the simple direct proportionality between the first order hyperfine splitting due to proton N and the zero order unpaired spin density at carbon atom N. The first order splitting  $a_N^{(1)}$  is negative since  $\rho_N^{(0)}$  is positive and  $(a_{CH}^0)_{MO}$  is negative.

A critical examination of the various approximations that have been used in obtaining equation 50 certainly does suggest several possible sources of error in this equation. Many of these approximations involve quantitative details which make difficult an a priori quantitative calculation of  $(a_{CH}^0)_{MO}$ , but which do not invalidate the simple linear relation in equation 1. These approximations are of minor importance in the present work. Other approximations - e. g., the assumed constancy of  $\Delta E_{2N, 1}$  - might lead to an apparent lack of constancy in Q values for different CH bonds, which in turn might conceivably lead in extreme cases to errors in electron densities of, say, 10 - 20%. Rather than errors of this sort, one is primarily concerned with possible order-of-magnitude errors. It is felt that the only likely case of order-of-magnitude deviations from the semi-empirical form of equation 50, i. e., equation 1, would arise in instances where  $\rho_N^{(0)} = 0$  and where the observed  $a_N$  is not zero. The relation  $\rho_N^{(0)} = 0$  will always arise when  $\pi_\lambda$  has a node passing through carbon atom N and proton N, in addition to the node which passes through the plane of symmetry of all the carbon atoms. Several indirect spin exchange coupling processes can give a finite  $a_N$  even when  $\rho_N^{(0)} = 0$ . It is proposed

that, as a rule, when  $\rho_N^{(0)} = 0$ , and finite values of  $a_N$  are observed, the principal contributions to  $a_N$  will still arise from unpaired spin density at carbon atom N. This unpaired spin density at carbon atom N in this case arises from  $\pi$ - $\pi$  configuration interaction.

The unpaired spin density at any carbon atom N can be written as a sum of terms,

$$\rho_N = \rho_N^{(0)} + \rho_N^{(1)} + \dots \quad (53)$$

where  $\rho_N^{(0)} = |a_{N\lambda}|^2$ . One is here concerned with a particular carbon atom,  $N = \bar{N}$ , for which  $|a_{\bar{N}\lambda}|^2 = 0$  and  $\rho_{\bar{N}}^{(0)} = 0$ . In this case there is also no first order hyperfine splitting,  $a_{\bar{N}}^{(1)} = 0$ , because there is no first order mixing of  $\psi_{2\bar{N}}^0$  with  $\psi_1^0$  according to equations 40, 42, and 46; that is,  $\eta_{2\bar{N}}^{(1)} = 0$ . Thus, one must seek higher order electron interactions which lead to unpaired spin density at  $\bar{N}$ , and which lead to a finite hyperfine splitting due to proton  $\bar{N}$ .

Consider the  $\pi$ -electron excited configurations  $\psi_4^0$ ,  $\psi_5^0$ , and  $\psi_6^0 - \psi_{10}^0$ .\*

$$\psi_4^0 = A \sigma \sigma \pi_u \pi_v \pi_\lambda \frac{1}{\sqrt{6}} a\beta \left\{ 2a\alpha\beta - a\beta\alpha - \beta\alpha\alpha \right\} \quad (54)$$

$$\psi_5^0 = A \sigma \sigma \pi_u \pi_v \pi_\lambda \frac{1}{\sqrt{2}} a\beta \left\{ a\beta\alpha - \beta\alpha\alpha \right\} \quad (55)$$

---

\* Since our calculations depend only upon the  $N^{\text{th}}$   $\sigma$ -bond, we shall, for simplicity, drop the subscript N from the notation describing the  $\sigma$ -electron functions in the following considerations.

$$\psi_j^0 \quad (j = 6 - 10) = A \sigma \sigma^* \pi_u \pi_\nu \pi_\lambda \Gamma_j \quad (56)$$

These states are arbitrary except that they are assumed to have the proper symmetry to mix with  $\psi_1^0$ .<sup>\*</sup> The functions  $\psi_j^0$ ,  $j = 6 - 10$ , correspond to the five doublet spin functions,  $\Gamma_j$ , for the doubly excited configuration shown in equation 56.<sup>\*\*</sup> The  $\pi$ -electron configuration interaction mixes these states with  $\psi_1^0$ :

$$\Psi = \psi_1^0 + (\eta_2 \psi_2^0 + \eta_3 \psi_3^0) + \eta_4 \psi_4^0 + \eta_5 \psi_5^0 + \sum_{j=6}^{10} \eta_j \psi_j^0 \quad (57)$$

where, as before,

$$\eta_i^{(1)} = - \frac{H_{i1}}{\Delta E_{i1}} \quad (58)$$

and, in particular,

$$H_{41} = - \frac{3}{\sqrt{6}} \langle \pi_\nu \pi_\lambda \left| \frac{e^2}{r} \right| \pi_\lambda \pi_u \rangle \quad (59)$$

Configuration  $\psi_4^0$  has the important effect of giving rise to unpaired electron density at carbon atom  $\bar{N}$ ,

\* We omit single  $\pi$ -electron excited state functions such as

$$\psi = A \sigma \sigma \pi_\gamma \quad \gamma \neq \lambda$$

since it can easily be shown that their contribution to the spin density and hyperfine splitting are negligible in the special case ( $a_{\bar{N}\lambda} = 0$ ) being treated above as well as in the zero order approximation.

\*\* See Appendix I, Part II.



$$\rho_{\bar{N}}^{(0)} = \langle \Psi_1^0 | \rho_N | \Psi_1^0 \rangle = 0 \quad (60)$$

$$\rho_{\bar{N}}^{(1)} = 2\eta_4 \langle \Psi_1^0 | \rho_N | \Psi_4^0 \rangle \quad (61)$$

$$= 2\eta_4 \left( \frac{2}{\sqrt{6}} a_{\bar{N}\nu} a_{\bar{N}u} \right) \quad (62)$$

The first order spin densities  $\rho_{\bar{N}}^{(1)}$  can be either positive or negative.

This can be seen by noting that

$$\sum_N \rho_N^{(1)} = \frac{4}{\sqrt{6}} \eta_4 \sum_N a_{\bar{N}\nu} a_{\bar{N}u} = 0 \quad (63)$$

The sum on the right side is zero because of the orthogonality of  $\pi_u$  and  $\pi_\nu$ . The total spin density at  $\bar{N}$ ,  $\rho_{\bar{N}}$ , can therefore be positive or negative, since  $\rho_{\bar{N}}^{(0)} = 0$ . The contribution of the other configurations to the density at carbon atom  $\bar{N}$  may be neglected.

It has been shown that configuration  $\Psi_4^0$  gives unpaired spin density at carbon atom  $\bar{N}$ , and it is now shown that configuration  $\Psi_4^0$  leads to a second order hyperfine splitting due to proton  $\bar{N}$ ; i. e.,  $a_{\bar{N}}^{(2)} \neq 0$ . Second order mixing between  $\Psi_1^0$ ,  $\Psi_2^0$  and  $\Psi_4^0$  puts some of the function  $\Psi_2^0$  into the ground state wave function; the amount of  $\Psi_2^0$  is given by the second order constant  $\eta_2^{(2)}$ .

$$\eta_2^{(2)} = \frac{H_{24} H_{41}}{\Delta E_{21} \Delta E_{41}} - \frac{H_{11} H_{21}}{(\Delta E_{21})^2} \quad (64)$$

$$= -\eta_4^{(1)} \frac{H_{24}}{\Delta E_{21}} \quad (65)$$

where

$$H_{24} (= H_{2\bar{N}, 4}) = - \langle \sigma_{\bar{N}}^* \pi_u \left| \frac{e^2}{r} \right| \pi_\nu \sigma_{\bar{N}} \rangle \quad (66)$$

$$= - a_{\bar{N}u} a_{\bar{N}\nu}^J \quad (67)$$

Thus, there will be a contribution to the hyperfine splitting  $a_{\bar{N}}^{(2)}$  of the form

$$(a_{\bar{N}}^{(2)})_{\psi_2^0} = \frac{2}{\sqrt{6}} \eta_2^{(2)} a_H^0 \frac{1}{\sqrt{1 - S_0^2}} \quad (68)$$

The remainder of  $a_{\bar{N}}^{(2)}$  will come from the cross terms between  $\psi_4^0$ ,  $\psi_5^0$  and  $\psi_6^0 - \psi_{10}^0$ . It will now be shown that the sum of these contributions is equal to  $(a_{\bar{N}}^{(2)})_{\psi_2^0}$ , so that the final result will be

$$a_{\bar{N}}^{(2)} = 2 (a_{\bar{N}}^{(2)})_{\psi_2^0} \quad (69)$$

Express the ground state function as

$$\Psi = (\psi_1^0 + \epsilon \psi_4^0 + \epsilon' \psi_5^0) + \sum_j' c_j \psi_j^0 \quad (70)$$

where the primed summation indicates that the sum is over all states except  $j = 1, 4, 5$ , i.e., the  $\sigma$ - $\pi$  and  $\sigma$  excited configurations. In

equation 70 the first approximation to the ground state wave function has been taken as  $\Psi_1^0 + \epsilon \Psi_4^0 + \epsilon' \Psi_5^0$  where

$$\epsilon = \eta_4^{(1)} \quad ; \quad \epsilon' = \eta_5^{(1)} \quad (71)$$

$$c_j = \frac{-\langle \Psi_1^0 + \epsilon \Psi_4^0 + \epsilon' \Psi_5^0 | H | \Psi_j^0 \rangle}{\Delta E_j} \quad (72)$$

and

$$\Delta E_j \approx \Delta E_{j1} = H_{jj} - H_{11} \quad (73)$$

One is here concerned with contributions to  $\delta_N$  of order  $\epsilon$  or  $\epsilon'$ .\*

Since

$$\langle \Psi_1^0 + \epsilon \Psi_4^0 + \epsilon' \Psi_5^0 | \delta_N | \Psi_1^0 + \epsilon \Psi_4^0 + \epsilon' \Psi_5^0 \rangle = 0 \quad (74)$$

to this order of magnitude,

$$\delta_N = -2 \sum_j \langle \Psi_1^0 + \epsilon \Psi_4^0 + \epsilon' \Psi_5^0 | H | \Psi_j^0 \rangle \langle \Psi_j^0 | \delta_N | \Psi_1^0 + \epsilon \Psi_4^0 + \epsilon' \Psi_5^0 \rangle \frac{1}{\Delta E_{j1}} \quad (75)$$

Because of the large difference in excitation energies of the  $\sigma$  and  $\pi$  electrons, one may approximate  $\Delta E_{21} \approx \Delta E_{31} \approx \Delta E_{61} \approx \dots \approx \Delta E_{10,1}$ ,

---

\* Since  $H_{21} = 0$  for the case a  $\overline{N\lambda} = 0$ , there will be no terms in  $\delta_N$  of lower order.

where  $\Delta E_{21} \gg \Delta E_{41} \approx \Delta E_{51}$ ; thus,  $\Delta E_{j1} = (\Delta E)$  may be treated as a constant and may be removed from the summation in equation 75.

Furthermore, because of equation 74, the sum in equation 75 may now be extended over all states. Thus,

$$\delta_N = \frac{-2}{(\Delta E)} \sum_i \langle \Psi_1^0 + \epsilon \Psi_4^0 + \epsilon' \Psi_5^0 | H | \Psi_i^0 \rangle \langle \Psi_i^0 | \delta_{-N} | \Psi_1^0 + \epsilon \Psi_4^0 + \epsilon' \Psi_5^0 \rangle \quad (76)$$

Retaining terms to order  $\epsilon$  or  $\epsilon'$  one obtains

$$\delta_N = \frac{-2}{(\Delta E)} \sum_i \left\{ \langle \Psi_1^0 | H | \Psi_i^0 \rangle \langle \Psi_i^0 | \delta_{-N} | \epsilon \Psi_4^0 + \epsilon' \Psi_5^0 \rangle + \langle \epsilon \Psi_4^0 + \epsilon' \Psi_5^0 | H | \Psi_i^0 \rangle \langle \Psi_i^0 | \delta_{-N} | \Psi_1^0 \rangle \right\} \quad (77)$$

which, because the sum extends over all states, simplifies to give

$$\delta_N = \frac{-2}{(\Delta E)} \left\{ \langle \Psi_1^0 | H \delta_{-N} | \epsilon \Psi_4^0 + \epsilon' \Psi_5^0 \rangle + \langle \epsilon \Psi_4^0 + \epsilon' \Psi_5^0 | H \delta_{-N} | \Psi_1^0 \rangle \right\} \quad (78)$$

$$= \frac{-4}{(\Delta E)} \langle \Psi_1^0 | H \delta_{-N} | \epsilon \Psi_4^0 + \epsilon' \Psi_5^0 \rangle \quad (79)$$

It is seen then that the two terms in equation 77 contribute equal amounts to  $\delta_N$  (and  $a_N$ ); the first term yields

$$\frac{-2}{(\Delta E)} \sum_{i=6}^{10} \langle \Psi_1^0 | H | \Psi_i^0 \rangle \langle \Psi_i^0 | \delta_{-N} | \epsilon \Psi_4^0 + \epsilon' \Psi_5^0 \rangle \quad (80)$$

and the second term a contribution

$$\frac{-2}{(\Delta E)} \langle \epsilon \Psi_4^0 + \epsilon' \Psi_5^0 | H | \Psi_2^0 \rangle \langle \Psi_2^0 | \delta_{-N} | \Psi_1^0 \rangle \quad (81)$$

which, since

$$\langle \Psi_5^0 | H | \Psi_2^0 \rangle = 0 \quad (82)$$

is equal to

$$\frac{-2\epsilon}{(\Delta E)} \langle \Psi_4^0 | H | \Psi_2^0 \rangle \langle \Psi_2^0 | \delta_{-N} | \Psi_1^0 \rangle \quad (83)$$

Taking  $(\Delta E) = \Delta E_{21}$ , it is easily seen that the contribution to  $a_N^{(2)}$  of the above term is simply  $(a_N^{(2)}) \Psi_2^0$ :

$$\begin{aligned} & \frac{-2\epsilon}{(\Delta E)} \langle \Psi_4^0 | H | \Psi_2^0 \rangle \langle \Psi_2^0 | \delta_{-N} | \Psi_1^0 \rangle \\ &= \frac{2 H_{41}}{\Delta E_{41}} \frac{H_{24}}{\Delta E_{21}} \langle \Psi_2^0 | \delta_{-N} | \Psi_1^0 \rangle \end{aligned} \quad (84)$$

$$= 2 \eta_2^{(2)} \langle \Psi_2^0 | \delta_{-N} | \Psi_1^0 \rangle \quad (85)$$

Thus, the equality in equation 69 has been proved and the cumbersome manipulation of the five five-particle doublet spin functions has been

avoided.\* From equations 68 and 69,

$$a_{\bar{N}}^{(2)} = \frac{4}{\sqrt{6}} \eta_2^{(2)} a_{\text{H}}^{\circ} \frac{1}{\sqrt{1 - S_o^2}} \quad (86)$$

$$= \frac{4}{\sqrt{6}} \eta_4^{(1)} \frac{a_{\bar{N}v} a_{\bar{N}u} J}{\Delta E_{21}} \frac{a_{\text{H}}^{\circ}}{\sqrt{1 - S_o^2}} \quad (87)$$

$$= -\frac{1}{2} \rho_{\bar{N}}^{(1)} \frac{J_{\text{ph}} - J_{\text{ps}}}{\Delta E_{21}} \frac{a_{\text{H}}^{\circ}}{1 - S_o^2} \quad (88)$$

$$= \rho_{\bar{N}}^{(1)} (a_{\text{CH}}^{\circ})_{\text{MO}} \quad (89)$$

One sees, therefore, by comparing equations 89 with equations 50 and 1, that even when  $\rho_{\bar{N}}^{(0)} = 0$  the observed hyperfine splitting can be used to estimate  $\rho_{\bar{N}}$  using equation 89 with  $(a_{\text{CH}}^{\circ})_{\text{MO}}$  set equal to  $Q$ . In the general case

$$a_{\bar{N}}^{(1)} + a_{\bar{N}}^{(2)} = (\rho_{\bar{N}}^{(0)} + \rho_{\bar{N}}^{(1)}) (a_{\text{CH}}^{\circ})_{\text{MO}} \quad (90)$$

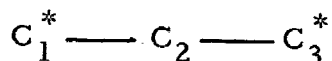
It is to be noted that the results in equations 89 or 90 are valid no matter how many  $\pi$ -electron configurations are included in the calculations, providing the mixing is first order.

---

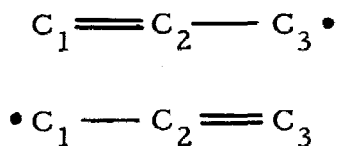
\* These calculations were carried out explicitly and gave exactly the indicated result. See Appendix I, Part II.

## DISCUSSION

In the present work, molecular orbital theory has been used to show that there exist relatively simple relations between calculated unpaired spin distributions in  $\pi$ -electron radicals and indirect proton hyperfine splittings. The linear relation given by equation 1 was derived in the first instance assuming the  $\sigma$ - $\pi$  exchange coupling to be first order. In the special case  $a_{\overline{N}\lambda} = 0$ , the linear relation was shown to still be exact, assuming that the  $\pi$ - $\pi$  configuration interaction could be treated as a first order perturbation on the  $\pi$ -part of the wave functions and that the excitation energies of the  $\sigma$ - $\pi$  excited states were all approximately the same and much larger than those of the  $\pi$ -excited states. A generalized treatment of this subject has been given (10) which treats arbitrary  $\sigma$ - $\sigma$  and  $\pi$ - $\pi$  interaction provided an average  $\Delta E$  can be assumed for the  $\sigma$ - $\pi$  excited states. This treatment has the advantage of not having to assume weak  $\pi$ - $\pi$  configuration interaction, an assumption often made but open to serious question. The problem may be illustrated by a comparison of spin densities in odd alternate hydrocarbons as calculated from valence bond theory, and molecular orbital theory under the assumption of weak  $\pi$ - $\pi$  configuration interaction. In odd alternate hydrocarbons Hückel  $\pi$ -MO theory puts positive spin density at each "starred" carbon atom. First order configuration interaction puts negative spin density at each of the unstarred atoms. For example, in the allyl radical,



$\rho_1^{(0)} = \rho_3^{(0)} = \frac{1}{2}$ ,  $\rho_2^{(0)} = 0$ . One can easily show - using molecular orbitals for this odd alternate system and equation 62 - that  $\pi$ - $\pi$  configuration interaction puts negative spin density at carbon atom  $N = 2$ . In the present work it has been assumed that this configuration interaction is weak, and this implies  $|\rho_2^{(1)}| \ll 1$ . On the other hand, one can easily show that resonance between the two simple valence bond structures



gives spin densities  $\rho_1 = \rho_3 = +\frac{2}{3}$ ,  $\rho_2 = -\frac{1}{3}$ . If the  $\pi$ - $\pi$  configurational interaction effects are actually as large as is implied by this simple valence bond calculation, then it is clear that the theoretical development given in the present work must be carried to higher order to describe the quantitative relation between spin density and proton hyperfine splittings.

On the experimental side, linearity between spin density at a carbon atom and the associated proton hyperfine splitting can only be tested by comparisons of the best theoretical values for the spin densities and the observed hyperfine splittings. At the present time a value of  $Q = -30 \pm 5$  gauss (and equation 1) does a satisfactory job of correlating calculated and "observed" spin densities in a number of even alternate hydrocarbons (Table 1). It is important to point out, however, that such comparisons require a detailed analysis of observed



TABLE 1

Apparent Q-values for different protons in aromatic radicals

Radical	Proton hyperfine splitting (gauss)	Molecular orbital density (0) $\rho_N$	Apparent Q (gauss)	Reference
benzene anion	TS* = 22.4	$\Sigma = 1.00$	22.5	15
naphthalene anion				16, 17
$\alpha$ -protons	5.01	0.18	28	
$\beta$ -protons	1.79	0.068	26	
biphenyl anion	TS = 21.0	$\Sigma = 0.754$	28	17
anthracene anion	TS = 26.1	$\Sigma = 0.967$	27	17
anthracene cation	TS = 31.5	$\Sigma = 0.967$	33	18
tetracene anion	TS = 24.7	$\Sigma = 0.950$	25	18
tetracene cation	TS = 29.0	$\Sigma = 0.950$	31	18
p-benzosemi-quinone anion	2.37	0.078	30	19, 20
o-benzosemi-quinone anion				19, 20
o-protons	1.0	0.049	20	
m-protons	4.0	0.089	45	

\* total spread

hyperfine structure. That is, the "total spread" of a hyperfine multiplet spectrum together with the total calculated spin density on carbon atoms with attached protons cannot be used to test the constancy of  $Q$ , since such an approach neglects the presence of negative spin densities.

To some extent purely experimental effects may be used to test the theoretical picture of indirect proton hyperfine interactions which has been developed in the present work. Negative proton hyperfine coupling constants for positive spin densities are an outstanding feature of the theory and can be checked from proton resonance shifts. Preliminary work on the interpretation of proton resonance shifts in nickelocene supports this idea of a negative paramagnetic nuclear shift (21). Negative spin densities which arise from  $\pi$ - $\pi$  configuration interaction (which lead to positive hyperfine coupling constants) should be observable as "normal" paramagnetic proton shifts.

## APPENDIX I

The results of the calculations involving the first term in equation 77 (i. e., equation 80) are given here. A set of five-particle doublet spin functions was derived using the methods of simple valence bond theory (22); linear combinations were taken to construct the orthogonal and normalized set  $\Gamma_j$ . Corresponding to the configuration given in equation 56, these spin functions are:

$$\Gamma_6 = \frac{1}{2} (\alpha\beta\alpha\beta\alpha - \alpha\beta\beta\alpha\alpha - \beta\alpha\alpha\beta\alpha + \beta\alpha\beta\alpha\alpha) \quad (\text{A-1})$$

$$\Gamma_7 = \frac{1}{2\sqrt{3}} (2\alpha\beta\alpha\alpha\beta - 2\beta\alpha\alpha\alpha\beta - \alpha\beta\alpha\beta\alpha - \alpha\beta\beta\alpha\alpha + \beta\alpha\alpha\beta\alpha + \beta\alpha\beta\alpha\alpha) \quad (\text{A-2})$$

$$\Gamma_8 = \frac{1}{2\sqrt{3}} (2\alpha\alpha\beta\alpha\beta - 2\alpha\alpha\beta\beta\alpha - \alpha\beta\alpha\alpha\beta + \alpha\beta\alpha\beta\alpha - \beta\alpha\alpha\alpha\beta + \beta\alpha\alpha\beta\alpha) \quad (\text{A-3})$$

$$\Gamma_9 = \frac{1}{6} (2\alpha\beta\beta\alpha\alpha - \alpha\beta\alpha\beta\alpha - \beta\alpha\alpha\beta\alpha + 2\beta\alpha\beta\alpha\alpha - \alpha\beta\alpha\alpha\beta - \beta\alpha\alpha\alpha\beta - 2\alpha\alpha\beta\alpha\beta - 2\alpha\alpha\beta\beta\alpha + 4\alpha\alpha\alpha\beta\beta) \quad (\text{A-4})$$

$$\Gamma_{10} = \frac{\sqrt{2}}{6} (-\alpha\beta\alpha\beta\alpha - \alpha\beta\beta\alpha\alpha - \beta\alpha\alpha\beta\alpha - \beta\alpha\beta\alpha\alpha - \alpha\beta\alpha\alpha\beta - \beta\alpha\alpha\alpha\beta + \alpha\alpha\beta\alpha\beta + \alpha\alpha\beta\beta\alpha + \alpha\alpha\alpha\beta\beta + 3\beta\beta\alpha\alpha\alpha) \quad (\text{A-5})$$

The following results were obtained for the non-zero hyperfine splitting and electronic matrix elements:

$$2 \langle \Psi_4^0 | \delta_{-N} | \Psi_8^0 \rangle = \sqrt{2} \sigma(0) \sigma^*(0) \quad (\text{A-6})$$

$$2 \langle \Psi_4^0 | \delta_{-N} | \Psi_9^0 \rangle = \frac{2}{\sqrt{6}} \sigma(0) \sigma^*(0) \quad (\text{A-7})$$

$$2 \langle \Psi_5^0 | \delta_{-N} | \Psi_8^0 \rangle = -\frac{2}{\sqrt{6}} \sigma(0) \sigma^*(0) \quad (\text{A-8})$$

$$2 \langle \Psi_5^0 | \delta_{-N} | \Psi_9^0 \rangle = \sqrt{2} \sigma(0) \sigma^*(0) \quad (\text{A-9})$$

$$\langle \Psi_1^0 | H | \Psi_8^0 \rangle = -\frac{3}{2\sqrt{3}} J a_{\bar{N}u} a_{\bar{N}v} \quad (\text{A-10})$$

$$\langle \Psi_1^0 | H | \Psi_9^0 \rangle = -\frac{J}{2} a_{\bar{N}u} a_{\bar{N}v} \quad (\text{A-11})$$

Equation 80 thus yields

$$\frac{4}{\sqrt{6}} \eta_4^{(1)} a_{\bar{N}u} a_{\bar{N}v} \frac{J \sigma(0) \sigma^*(0)}{\Delta E_{21}} \quad (\text{A-12})$$

where the terms involving  $\eta_5^{(1)}$  have cancelled each other, and, as before, the relation  $\Delta E_{81} \approx \Delta E_{91} \approx \Delta E_{21}$  has been assumed. The contribution to  $a_{\bar{N}}^{(2)}$  of equation 80 is thus

$$(a_{\bar{N}}^{(2)})_{\text{eq. 80}} = \frac{2}{\sqrt{6}} \eta_4^{(1)} \frac{a_{\bar{N}v} a_{\bar{N}u} J}{\Delta E_{21}} \frac{a_H^0}{\sqrt{1 - S_o^2}} \quad (\text{A-13})$$

which (from equation 87) is seen to be exactly one half of  $a_{\bar{N}}^{(2)}$  as proved in equations 70 - 83.

## REFERENCES TO PART II

1. H. M. McConnell, Ann. Rev. Phys. Chem. 8, (1957), in press.
2. H. M. McConnell, J. Chem. Phys. 24, 764-766 (1956).
3. H. M. McConnell, J. Chem. Phys. 24, 632 (1956).
4. R. Bersohn, J. Chem. Phys. 24, 1066-1070 (1956).
5. S. I. Weissman, J. Chem. Phys. 25, 890-891 (1956).
6. B. Venkataraman, G. K. Fraenkel, J. Chem. Phys. 24, 737-740 (1956).
7. H. M. McConnell, D. B. Chesnut, J. Chem. Phys., (1957), in press.
8. P. Brovetto, S. Ferroni, Il Nuovo Cimento 5, 142-153 (1957).
9. S. I. Weissman, J. Chem. Phys. 22, 1378-1379 (1954).
10. H. M. McConnell, D. B. Chesnut, J. Molecular Spectroscopy, (1957), in press.
11. H. S. Jarrett, J. Chem. Phys. 25, 1289-1290 (1956).
12. S. L. Altman, Proc. Royal Soc. (London) A210, 327-354 (1951).
13. H. H. Voge, J. Chem. Phys. 16, 984-986 (1948).
14. H. M. McConnell, J. Molecular Spectroscopy, (1957), in press.
15. S. I. Weissman, T. R. Tuttle, Jr., E. de Boer, J. Phys. Chem. 61, 28-31 (1957).
16. T. R. Tuttle, Jr., R. L. Ward, S. I. Weissman, J. Chem. Phys. 25, 189 (1956).
17. E. de Boer, J. Chem. Phys. 25, 190 (1956).
18. S. I. Weissman, E. de Boer, J. J. Conradi, J. Chem. Phys. 26, 963-964 (1957).

19. B. Venkataraman, G. K. Fraenkel, J. Amer. Chem. Soc. 77, 2707-2713 (1955); J. Chem. Phys. 23, 588-589 (1955).
20. R. Hoskins, J. Chem. Phys. 23, 1975-1976 (1955).
21. H. M. McConnell, private communication, May, 1957.
22. L. Pauling, E. B. Wilson, Introduction to Quantum Mechanics, McGraw-Hill Book Company, Inc., 1935, pp. 374-377.

## PROPOSITIONS

1. \* A simple analytical representation of atomic scattering factors for use on high speed digital computers has been found. A program has been written (for the ElectroData Corporation Datatron digital computer) to give an optimum fit for the desired f-curve. A test case (nitrogen f-curve) has yielded surprisingly good results.

2. A simple relation between covalent single-bond radii ( $r$ ) and electronegativities ( $x$ ) has been found of the form

$$x/r = \alpha x + \beta$$

where  $\alpha$  and  $\beta$  are constants characteristic of the particular row of the periodic table involved. A comparison of the above expression and the electronegativity scales of Gordy (1) and Mulliken (2) yields a rather interesting result.

3. A useful approach to the determination of accurate film factors in crystal structure intensity measurements is proposed.

4. (a). Some suggestions are made concerning the publication of crystal structure data and results.

(b). A study should be made on the relative merits and effects of different weighting schemes. In particular, an analysis of the least-squares procedure as a function of  $\Delta r$  should be undertaken.

---

\* This problem was suggested to the author by Dr. Marsh.

- (c). The importance of difference-map refinement relative to the usual least-squares treatment in the early stages of a three dimensional refinement is emphasized (3).
5. An experiment is suggested to evaluate the theory proposed by Piez and Eagle (4) to explain the  $C^{14}$  isotope effect on the ion-exchange chromatography of amino acids.
  6. Several suggestions are made concerning the educational program at California Institute of Technology.
  7. A quick, simple method is proposed for estimating electron spin densities (5) in planar aromatic (odd-alternate) radicals using the methods of valence bond theory.
  8. The experiment of Berenblum and Haran (6) does not unambiguously prove the proposed two-stage mechanism (7) of chemically induced carcinogenesis as claimed.
  9. The Schomaker-Stevenson (8) empirical correction to the additivity rule for single-bond distances can be plausibly explained starting with Pauling's (9) argument concerning the effect of electrical charge on covalent radii.
  10. It is proposed that a file be set up in which reprints of recent department work may be made readily available. The advantages of such a system are discussed.



## REFERENCES TO PROPOSITIONS

1. W. Gordy, Phys. Rev. 69, 604-607 (1949).
2. R. S. Mulliken, J. Chem. Phys. 2, 782-793 (1934); 3, 573-591 (1935).
3. D. B. Chesnut, Thesis, California Institute of Technology, 1958, Part I, pg. 13.
4. K. A. Piez, H. Eagle, J. Amer. Chem. Soc. 78, 5284-5287 (1956).
5. D. B. Chesnut, Thesis, California Institute of Technology, 1958, Part II.
6. I. Berenblum, H. Haran, Brit. J. Cancer 9, 268-271 (1955).
7. G. Wolf, Chemical Induction of Cancer, Harvard Univ. Press, 1952, ff 80.
8. V. Schomaker, D. P. Stevenson, J. Amer. Chem. Soc. 63, 37-40 (1941).
9. L. Pauling, The Nature of the Chemical Bond, Cornell Univ. Press, 1948, pp. 169-170.